A theoretical study of ionic liquids using analytical theory and molecular dynamics simulation

by

Hualin Li

A dissertation submitted to the Graduate Faculty in Chemistry in partial fulfillment of the requirements for the degree of Doctor of Philosophy, The City University of New York

2011

This manuscript has been read and accepted for the
Graduate Faculty in Chemistry in satisfaction of the
dissertation requirement for the degree of Doctor of Philosophy

Prof. Mark Kobrak

Date

Chair of Examining Committee

Prof. Mahesh Lakshman

Date

Executive Officer

Prof. Mark Kobrak

Prof. Andrzej Jarzecki

Prof. Steve Greenbaum

Supervisory Committee

The City University of New York

ABSTRACT

Title of Thesis: A theoretical study of ionic liquids using analytical theory and molecular dynamic simulation

by

Hualin Li

Thesis directed by: Mark Kobrak, Professor of
Department of Chemistry of City University
of New York

In a series of theoretical analyses and simulation studies, we explore the relationship between ionic structure and liquid dynamics in room-temperature ionic liquids (ILs). As a framework, we define an ionic property we call the Charge Lever Moment (CLM) based on earlier theoretical work. We use the CLM to investigate ionic liquid dynamics and demonstrate a correlation between the CLM and IL viscosity. We extend this analysis using molecular dynamics simulation of a series of model molten salts with different intra-ionic charge distributions. These simulation clarify the relationship between charge distribution and ionic motion. We extend the analysis further with a thorough study using an instantaneous normal mode analysis in the model ILs, with the goal of investigating the roles of translational and rotational motion in IL dynamics.

ACKNOWLEDGMENTS

I am heartily thankful to my advisor, Prof.Mark Kobrak, whose encouragement, patience, and great support from the initial to the final level enabled me to develop an understanding of the subject while allowing me the room to work in my own way. I also thank my other committee members, Prof.Steven Greenbaum and Prof.Andrzej Jarzecki, for their thorough reviews and illuminating comments from proposal development to thesis writing. I also thank Professor Edward W. Castner, Dr. James F. Wishart, and Dr. Alison M. Funston for many helpful discussions.

I am grateful to the Chemistry program at Graduate Center and Chemistry Department at Brooklyn College of City University of New York, particularly the faculty and staff I have encountered during my study, for making the whole graduate experience enjoyable and productive.

Lastly, I offer my regards and appreciations to all of my family and friends who supported me in any respect during the completion of the project.

TABLE OF CONTENTS

LIST OF FIGURES

LIST OF TABLES

INTRODUCTION

The study of organic salts that are molten at low temperatures has been receiving more and more attention from researchers in the past decade. These systems are commonly referred to as room temperature ionic liquids (ILs), and possess a melting point less than 100°C. ILs are purely ionic systems at room temperature, which makes them very different from common molecular liquids in a number of ways. As a class, they mostly possess higher boiling points (Earle *et al.* 2006)and viscosities(Noda, Hayamizu, & Watanabe 2001) than molecular liquids, as well as having much larger electrochemical windows(Tokuda *et al.* 2005) and extremely low vapor pressures(Noda, Hayamizu, & Watanabe 2001). Research in understanding the microscopic structure(Canongia-Lopes, Deschamps, & Pádua 2004; Hayashi, Ozawa, & Hamaguchi 2003)and dynamics(Cang, Li, & Fayer 2003; Arzhantsev *et al.* 2006; Li *et al.* 2006) of ionic liquids has been increasing dramatically in recent years. Many of the favorable properties of ILs suggest that they may be environmentally sound alternatives to most traditional organic solvents to achieve "green chemistry". More research is under way that may enable their use in a huge range of synthetic, separatory and electrochemical processes(Welton 1999; Seddon 1997; Wasserscheid & Welton 2002; Dupont, de Souza, & Suarez 2002).

However, despite substantial research on ILs using both experimental(Huddleston *et al.* 2001; Tokuda *et al.* 2005) and theoretical methods(Urahata & Ribeiro 2004; 2005; Wang & Voth 2005), their structure and dynamics remain poorly understood. A detailed understanding of their physicochemical behavior based on a more exact microscopic picture will definitely facilitate their possible application.

The goal of this thesis is to use a combination of analytical theory and molecular dynamics (MD) simulation to investigate the ionic structure and dynamics of ILs at a mi-

croscopic level. The work also attempts to characterize the ILs empirically by correlating experimental results with theoretical studies.

Structures and physical properties of ionic liquids The huge number of known ILs can be divided into many categories. The "deep eutectic" systems composed of organic salts and molecular species have been reported,(Abbott *et al.* 2003)in which ionic complexation drives a lowering of the melting point. Some ionic systems are observed to be undergo covalent rearrangements in the melt,(Olivier-Bourbigou & Magna 2002; Chauvin & Olivier-Bourbigou 1995)creating complex equilibria that remain fluid to low temperature. For example, the ILs formed by the tetrachloroluminate anion will lead to an equilibrium with a dialuminum complex. Additionally, many ILs containing divalent or trivalent cations or anions are known to exist(Engel, Cohen, & Lall 2002),even though most of them have received less attention from researchers than monovalent ILs.

This thesis focuses on monovalent ILs with representative species of cations and anions given in Fig 1. The cations mainly include: alkylammonium, imidazolium, pyridinium, pyrrolidinium, and alkylphosphonium species, while the anions are usually smaller inorganic anions. A tentative explanation for ILs' low melting points relies on the large mismatch in ionic size and symmetry between the cations and anions, leading to prototypical "bad" crystals.

A brief overview of the macroscopic physical properties of ILs is given here. As per the definition of ILs mentioned above, ILs are usually defined to possess a melting point less than 100°C. It is reported that some (but few) species based on imidazolium and pyridinium cations have melting points as low as -80°C(Holbrey *et al.* 2003; Crosthwaite *et al.* 2005a). One IL property that may facilitate the some novel reactor designs is their extremely low vapor pressure, which makes them better organic solvents to achieve "green chemistry". But it must be noted that some species possess significant vapor pressures and

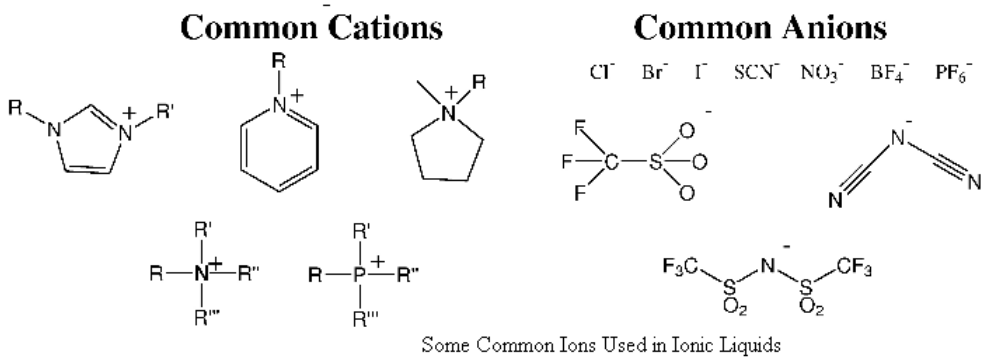

FIG. 1. Schematic of cations and anions in ILs.

may be distilled at elevated temperatures(Rebelo *et al.* 2005). The thermostability of ILs is good and varies between different species(Fox *et al.* 2005).

The miscibility of ionic liquids has been investigated(Dyson, Ellis, & Welton 2001; Tokuda *et al.* 2005; Aki, Scurto, & Brennecke 2006). Due to their different miscibility in water, the ILs can be divided broadly into two major categories: "hydrophilic" and "hydrophobic". The aqueous miscibility of ILs also depends on the temperature.

The transport properties of ILs have been the subject of much recent study(Okada 2001), not only because of their relevance to electrochemistry, but also because the high viscosities(from 30 to 10000 cP(Crosthwaite *et al.* 2005b)) ILs possess are an obstacle in their application in both laboratory and industrial processes. Usually, the viscosity will increase with increasing of molecular weight of the IL, which is in the same trend that appears in molecular liquids. However, it has been proved by many researchers that the ionic structure and configuration of the ion will also play an important role. We will go back to this subject and discuss this relationship in more detail in the later chapters.

Experimental studies of ionic liquids MacFarlane et.al (MacFarlane *et al.* 2002) reported a series of ionic liquids based on the imidazolium, ammonium, and pyrrolidinium salts of the dicyanamide ion, and observed that certain room-temperature ILs exhibit very low viscosities. They attributed this observation to the rigid asymmetric geometry of dicyanamide. This interesting phenomenon raises an important question: How does ionic liquids' chemical structure and configuration influence their properties?

The imidazolium−based ionic liquids have been investigated to determine their liquid structures by X-ray and Raman experiments. The association of aliphatic substituent groups is found to lead to segregation between ionic and aliphatic regions in ILs.(Katayanagi *et al.* 2004) The red edge effect (REE) in fluorescence phenomena also indicates microscopic spatial inhomogeneity. It is reported, based on the fluorescence spectra of chromophores solvated in imidazolium-based ILs, that the chromophore exists in different chemical environments, further evidence of inhomogeneity.(Mandal, Sarkar, & Samanta 2004)

Nanoscale domains in room temperature ionic liquids have been found by coherent anti−Stokes Raman spectroscopy.(Shigeto & Hamaguchi 2006) Xiao and Quitevis (Xiao *et al.* 2006) report the Kerr effect spectra of a binary mixture of ILs. They found that the Kerr effect spectra can be viewed as a sum of the spectra of individual liquids. They interpret this additivity to be evidence of the existence of nanoscale organization in the ILs. The microscopic domains in these two liquids preserve the distinctive motions associated with the spectra of each liquid.

Just as these studies provide strong evidence of spatial inhomogeneity in ILs, there is also evidence of dynamic inhomogeneity. It is widely accepted that the ions in ILs do not move independently and ionic motion is a very complicated process, leading to effects often interpreted as ion paring in ILs. This effect, which provides an important clue about the specific and nonspecific energetic interactions between ions, causes inhomogeneous

dynamics in the ILs.

Shirota and Castner(Shirota & Castner 2005a; Shirota *et al.* 2005; Shirota & Castner 2005b) also report some interesting Kerr effect results in ILs, by comparing the spectrum of an ionic liquid with an isoelectronic binary mixture of molecular liquid. They found that a much broader spectrum is observed in the IL sample, which is strong evidence of glassy or supercooled dynamics. Other optical Kerr effect experiments on ILs are reported by Hyun et.al(Hyun *et al.* 2002)and Cang et.al(Cang, Li, & Fayer 2003), and indicate that a bimodal distribution of intermolecular dynamics. This is further evidence of dynamical inhomogeneity in ILs.

Theoretical studies of ionic liquids In addition to experimental studies of ionic liquids, a large number of simulation and theoretical studies have explored the structure and dynamics of ILs. As we mention above, structural inhomogeneity has been an important finding in ILs. This observation is consistent with simulation results reported by Canongia−Lopes et al. (Canongia-Lopes & Pádua 2006; Canongia-Lopes, Gomes, & Pádua 2006) and Voth et al. (Wang & Voth 2005). Both of the these studies described the segregation of ILs into chemically distinct regions. The red edge effect is reproduced in simulation by Hu and Margulis (Hu & Margulis 2006a; 2006b), showing that different regions of the emission spectrum are associated with distinct distributions of solvent around the chromophore, providing further evidence of spatial inhomogeneity.

The dynamical inhomogeneity of ILs also affects the diffusive behavior of ions in ionic liquids. Urahata and Ribeiro(Urahata & Ribeiro 2005) and Margulis and Berne(Margulis, Stern, & Berne 2002) have reported that different time scales of ionic diffusion exist, meaning ions can diffuse rapidly over very small distances and then more slowly over longer time scales. These observations can be explained by a “cage” of counterions from which diffusing ions must escape. This is a characteristic of glasses and supercooled liq-

uids. Yan and Voth(Yan *et al.* 2004) also report that the electronic polarizability of ions can affect IL dynamics. Margulis et.al(Hu & Margulis 2006a) suggest that the spatial and dynamic inhomogeneity of ILs are related to more rapid motion of ions at the edges of certain spatial domains.

Although the issues described above are important, we have to come back to the question again: How does an ionic liquid's chemical structure influence its properties? This question has been touched on in this introduction by noting the features of ions that are dominant factors affecting the IL dynamics. However, we have not considered in detail how the distribution of charge and mass within an individual ion should influence the liquid properties of ILs. A better understanding to this question would benefit both laboratory research and industrial application of ionic liquids.

One of the obstacles in the application of ILs is their high viscosity. It is reported that by choosing the specific cation and anion, on the order of 10^5 varieties of ILs could be constructed .(Yan *et al.* 2004) Also it has been shown that viscosity, glass transition temperature, and other liquid properties can be controlled by chemically modifying the anion or cation of the ILs. Therefore, understanding the structure-property relationships of ILs may make it possible to design "ideal" liquids for a given task.

We first consider the Taylor series expansion of the electrostatic potential of the ions and develop a descriptor called the Charge Lever Moment(CLM) related to the distributions of charge and mass in an ion to describe this structure-property relationship.(Li *et al.* 2008)The principle of this analysis is that the dynamic response of the ion to an electric field generated by the motion of neighboring ions will play an important role in the ionic motion, and Coulombic coupling of rotational and translational motions can dramatically alter the time scale for transport properties such as ionic diffusion, viscous flow, and solvation dynamics. We use this new CLM formalism to interpret the relative viscosities of structurally analogous ILs and show that the value of the maximum CLM of an ion corre-

lates strongly with the viscosity of an IL made from that ion. However, this CLM formalism breaks down for highly flexible ions. What is more, certain structural features of the ions, such as the branching of alkyl substituents, apparently have significant effects on viscosity that are not properly accounted by this formalism.

The previous study mentioned above and the fact that liquid dynamics are generally relatively rapid in ILs composed of rigid asymmetric ions(MacFarlane *et al.* 2002; Mantz & Trulove 2002), all indicate that the charge distribution and symmetry of an ion will have a profound effect on liquid dynamics. With all these ideas in mind, we perform a series of molecular dynamics (MD) simulations(Li & Kobrak 2009) on ILs composed of rigid model ions which possess a high symmetry in mass distribution but may be either symmetric or asymmetric in their charge distribution. Both the structure and the dynamics of the liquids are studied to determine how variation in the charge distribution of the ions influences liquid behavior. The MD simulation results indicate that the liquid structures are not highly sensitive to ionic charge distribution. However, the dynamic properties are sensitive to the distribution of charge within the ions. It is found that a slower librational decay and faster translational diffusion appear in the asymmetric species, which indicates stronger Coulomb interactions coupling rotational and translational motion in asymmetric species. This is consistent with our earlier work on the CLM, where significant asymmetry in charge distribution with an ion is associated with a reduced viscosity. The role of quadrupolar coupling and other higher-order electrostatic terms is also considered.

The study above is extended through the performance of an instantaneous normal mode (INM)analysis. The INM spectrum is assembled, and the separate translational and rotational contribution to each instantaneous normal mode is calculated by computing the appropriate projectors from the eigenvectors. The results indicate that the rotational behavior of both model salts described by the INM approach is consistent with the MD simulation results introduced in chapter 2, while the translational motion is more complicated and will

be discussed in detail in section 3.3.2.

Chapter 1

THE RELATIONSHIP BETWEEN IONIC STRUCTURE AND VISCOSITY IN ROOM-TEMPERATURE IONIC LIQUIDS

abstract We investigate the relationship between ionic structure and viscosity in room-temperature ionic liquids.We build on an earlier theoretical work and derive an ionic property we call the charge lever moment (CLM) that provides insight on ionic liquid dynamics. We use electronic structure calculations to determine the CLM for ions in typical ionic liquids and demonstrate a correlation between this property and the experimental viscosities of ionic liquids. The relationship provides insight into the role of librational motion in ionic liquids in general, and the interpretation of Kerr effect experiments is discussed.

1.1 Introduction

Understanding the dynamical properties of ILs is an important goal for this field. It has been shown that viscosity, glass transition temperature, and other liquid properties can be controlled by chemically modifying the anion or cation of the IL,(Shirota & Castner 2005a) suggesting that physical properties can be optimized to a given application. Such optimization, however, requires an understanding of structure-property relationships.

Quantitative structure-property relationships (QSPRs) for a wide range of physical properties have been studied in molecular liquids.(Karelson 2000) Such studies typically involve analysis of the structures and experimentally measured properties of hundreds of different molecular liquids, and provide a high degree of accuracy in their predictions. There are unfortunately two major obstacles to the implementation of such techniques in ILs. The first is a shortage of experimental data. While a large number of IL species are known,(Wasserscheid & Welton 2002) characterization of their physical properties is incomplete. Even with the recent development of a comprehensive database on the subject,(Seddon 2005) the data set is far too sparse to support the level of sophistication employed in QSPR treatments of molecular liquids except in special cases.(Eike, Brennecke, & Maginn 2003; Varnek *et al.* 2007)

The second major obstacle to the development of QSPR for ILs is the need for new physical theories to identify the relevant variables. While the relevance of the parameters employed in QSPR treatments of molecular liquids is often not immediately clear, it can generally be understood with reference to simpler theories for molecular behavior. Before ILs can be treated effectively in QSPR, new theories must be developed that at least crudely identify the variables relevant to a given structure-property relationship. Indeed, Matsuda et al.(Matsuda *et al.* 2007) attempted to use a reverse design QSPR approach to model the conductivities and viscosities of ILs that deliberately avoids the inclusion of sophisticated ionic descriptors, and their results are consequently of limited utility in understanding ILs.

Here, we present a physically motivated theory that can be used to interpret the relative shear viscosities of two ILs. The theory relates the distributions of charge and mass in an ion to the dynamic response of the ion to the electric field generated by the motion of neighboring ions. Key to this analysis is the coupling of rotational and translational motions in neighboring ions. Since in at least some cases the rotational response of an ion is more rapid than the translational response, the mixing of these degrees of freedom can dramatically

alter the time scale for transport properties such as ionic diffusion, viscous flow, and solvation dynamics. A number of experimental techniques, such as Kerr spectroscopy, can give detailed insight into the dynamics of liquids. However, only a limited number of such studies are available for ILs, and the data set is too sparse to provide a good test of the theory. While we will discuss the application of the theory to the interpretation of Kerr effect experiments in Sec.1.3.3, we focus on analysis of the shear viscosities of ILs. These experiments are sufficiently simple that experimental data are reported for a large number of liquids, making a systematic comparative study possible. Moreover, given that the high shear viscosities typical of ILs are a stumbling block to their exploitation,(Crosthwaite *et al.* 2005a; Mantz & Trulove 2002) a better understanding of the relationship between IL structure and viscosity is of particular value to the field. Properties such as solvation dynamics(Arzhantsev *et al.* 2003) and conductivity have also been found to relate to viscosity in ILs, so the insight obtained in this study can be broadly applied. In the following two sections, we consider only the shear viscosity (henceforth referred to simply as viscosity). We consider the application of the theory developed here to Kerr effect spectra in Sec.1.3.3, but note that the more limited dataset makes the analysis less extensive.

1.2 Theory and Methodology

Liquid viscosity is a complex property, and any attempt to interpret it with reference to a single parameter must have a very limited expectation of success. QSPR treatments of viscosity in molecular liquids make use of eight to ten parameters to obtain reasonable agreement with experiment,(Kauffman & Jurs 2001; Suzuki, Ebert, & Schüürmann 2001) as even obvious relationships can be obscured by other variables. For example, the relationship between molecular mass and viscosity is generally accepted in molecular liquids, but the presence of hydrogen bonding and other intermolecular forces can make it diffi-

cult to prove the relationship. We must therefore approach the case of ILs with the goal of establishing a correlation between viscosity and the variable of interest for a homologous series of ions, where the variability in other parameters is minimized. Future work can make use of this correlation in more sophisticated QSPR treatments. In this paper, we present a model describing ionic motion in fused salts. We begin by reviewing some of our prior work using a simpler model, and then expand on this formalism. The result is a calculable ionic property termed the charge lever moment, and we demonstrate a correlation between this value and the observed experimental shear viscosity for three series of structurally homologous ILs.

1.2.1 The Charge Arm

The asymmetry of the distribution of mass and charge in an ion has been identified as an important determinant of liquid viscosity, and quantified with a quantity called the "charge arm."(Kobrak & Sandalow 2006) An empirical correlation between viscosity and charge arm was noted in that work. We review the construction of the charge arm below. The approach is based on the center of charge description of the ion,(Wangsness 1986)in which the electrostatic potential of a body is approximated in a Taylor series expansion, and the electrostatic potential is then assumed to be dominated by the lowest-order term in the expansion. This approach is exactly analogous to the derivation of the dipole moment for a neutral body. In charged bodies such as ions, however, the lowest-order term is the charge (monopole) moment, and the optimal low-order electrostatic description of the body is a point charge located at the maximum or minimum in the electrostatic field. This point R_{cq} is given by

$$R_{cq} = \sum_{i=1}^{N} \frac{q_i r_i}{Q} \tag{1.1}$$

where Q is the total charge on the body and q_i and r_i are the charge and location of the ith atomic site, respectively. In this representation, the dipole moment of the ion is rigorously zero, and further information on the details of the charge distribution is contained in the quadrupole moment and higher-order terms.

This has significant implications for dynamics. Consider a rigid spherical ion with a center of mass R_{cm} located at its geometric center and a center of charge R_{cq} that may either be equivalent to R_{cm} or displaced from it, as shown in Fig.1.1. If R_{cq} and R_{cm} are identical, as in a highly symmetric ion, rotation of the ion does not (to lowest order) alter its Coulomb interactions with neighboring ions. If the centers of mass and charge are displaced, however, the rotational motion of ions is coupled electrostatically.

Such coupling may have a dramatic impact on the dynamics of ILs. Both translational and rotational dynamics in ILs are notoriously slow, and correlations can persist on nanosecond time scales.(Arzhantsev *et al.* 2006; Hu & Margulis 2006a)However, in analyzing the molecular dynamics simulations of alkylimidazolium chloride ILs, Urahata and Ribeiro(Urahata & Ribeiro 2005) noted vastly different time scales for rotational response about different axes of the cation. They define an axis through the nitrogens of the imidazolium ring, which roughly parallels the alkyl substituent of the ring when it is extended in an all trans geometry. Relaxation for rotation of the ion about this axis is slow for the two species studied with less than 50% of the relaxation complete in the first 600 ps. In contrast, there is an extremely rapid component to the rotational response about the other axes, and in both cases 25% of the response is complete in the first 30 ps and 50% of the response complete within the first 100 ps. These vastly different rotational dynamics provide a clue as to the relationship between ionic structure and dynamics, and imply that coupling of translational and rotational motions could reduce the time scales for ionic diffusion and viscous flow.

As a point of reference, consider Fig.1.1 Given an isolated ion with nonequivalent

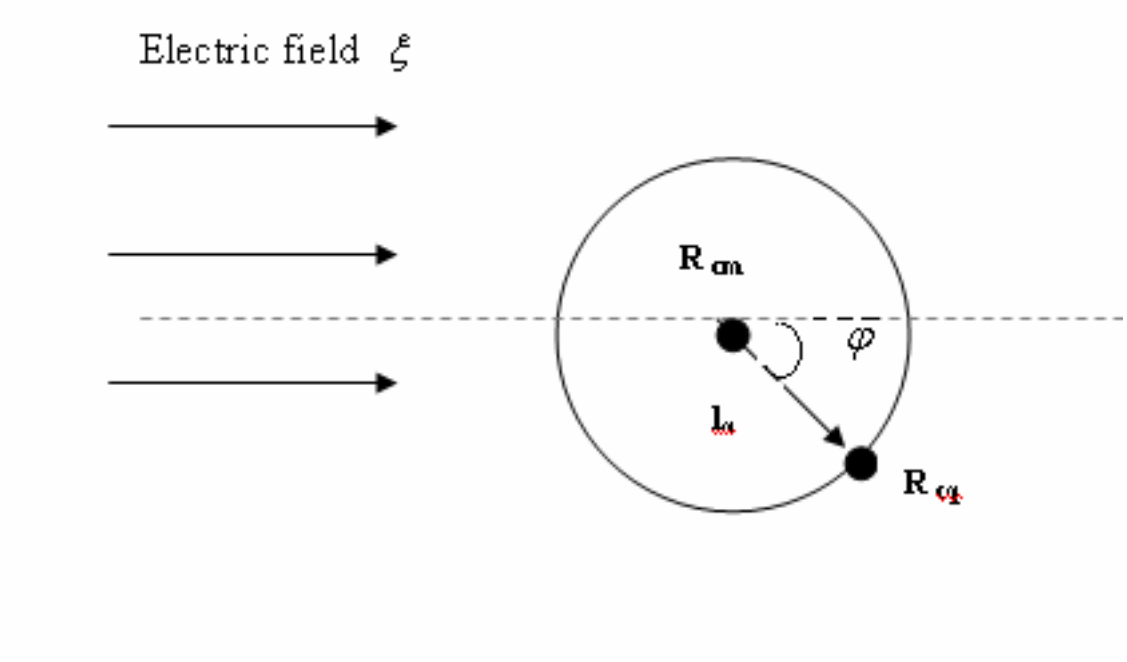

FIG. 1.1. Schematic of an ion interacting with an applied electric field.

centers of mass and charge, an applied electric field will lead to both translational and rotational acceleration of the ion, and the rate of angular acceleration will be determined by the distance between the centers of mass and charge as well as the moment of inertia. Considering the same ion in the condensed phase, one may view the applied electric field as resulting from the displacement of a neighboring ion in translational diffusion or viscous flow. The translational response of the ion is hindered by the presence of neighboring ions, and is apt to be very slow, as noted above. However, the rotational response of the ion makes it possible to reduce the interaction energy with the neighboring species more rapidly, potentially increasing the rate at which the neighboring ion can diffuse.

A complication to this picture is that IL dynamics are known to be highly collec-

tive,(Kobrak 2006; 2007; Urahata & Ribeiro 2006) with correlated ionic motions emerging even on subpicosecond time scales. These correlations are driven by long-ranged Coulomb interactions, implying that where the centers of mass and charge are displaced in ions, collective motion must include both rotational and translational components. The mixing of more rapid rotational dynamics with slower translational degrees of freedom will produce dynamics on a more rapid time scale than that which would emerge from purely translational dynamics. The effect is analogous to the mixing of local modes in the normal modes of intramolecular vibration; where coupling is strong, the incorporation of high frequency local modes into a normal mode increases the frequency of the collective vibration. Considering the isolated ion more quantitatively, the angular acceleration of a rigid spherical ion in response to an applied electric field of magnitude E (shown schematically in Fig. 1) is given by

$$\ddot{\phi} = -\frac{El_q \sin\phi}{I} \tag{1.2}$$

where I is the moment of inertia, ϕ is the angle between the applied field and the vector connecting R_{cm} and R_{cq}, and l_q is the magnitude of that vector. This equation is incorrect in Reference(Kobrak & Sandalow 2006), though the error does not affect subsequent derivations in that reference. It is clear from Eq. 1.2 that the magnitude $|Ql_q|$ represents a property of the ion that is proportional to the rate of librational response to an applied electric field. This quantity was labeled the charge arm,(Kobrak & Sandalow 2006) and was used to interpret the relative viscosities of sets of homologous ILs.

1.2.2 The CLM

While the charge arm approach proved sufficient for some limited interpretations of the relative viscosities of different liquids, it is too simple a formalism to permit deeper

investigation. As written, the charge arm does not include information on the moment of inertia of the ion, and so permits comparison only of ions of nearly equivalent mass. It also takes no account of ionic asymmetry. We therefore present a more sophisticated formulation that explicitly includes the ionic moments of inertia and the asymmetry of the ion. The components of the moment of inertia for an ion can be written

$$I_{ij} = I_{ji} = -\sum_{k=1}^{N} m_k i_k j_k, \tag{1.3}$$

$$I_{ii} = -\sum_{k=1}^{N} m_k(|r_k|^2 - i_k^2), \tag{1.4}$$

where m_k and r_k are the mass and position of the kth atom, respectively, and i and j are the Cartesian coordinates of the moment of inertia. The scalar variables i_k and j_k are the Cartesian components of r_k. The equations of motion for a rigid rotating body can be solved by diagonalizing the matrix I to obtain the principal axes of rotation for the body and the moment of inertia about each. This creates three degrees of rotational freedom that are not dynamically coupled.

We label these three axes $\mathbf{R_i}$ and the moments of inertia as I_i, and consider a force $\mathbf{F}$ applied to the body. The torque τ_i around the axis i is given by

$$\tau_i = \mathcal{R}_i \times \mathbf{F} \tag{1.5}$$

where $\mathcal{R}_i$ is the shortest vector from the ith axis to the point at which the force $\mathbf{F}$ is applied.

If we use the center of charge approximation for an ion of charge Q, the force associated with an applied electric field $\mathbf{E}$ is, to first order, localized at the center of charge. The torque on the body can be written as

$$\tau_i = \mathbf{L}_{q,i} \times (\mathbf{QE}) \tag{1.6}$$

where $\mathbf{L}_{q,i}$ is the shortest vector from the ith axis to the center of charge. This can be written as

$$\mathbf{L}_{q,i} = \mathbf{L}_q - (\mathbf{L}_q \cdot \mathbf{R}_i)\mathbf{R}_i \tag{1.7}$$

where $\mathbf{L}_q$is the vector connecting the center of mass to the center of charge. The configuration is shown schematically in Fig.1.2.

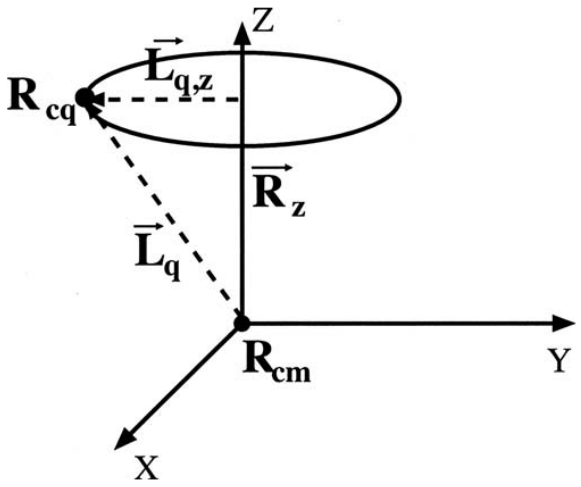

FIG. 1.2. Schematic of the CLM of an ion

In this construction, the angular acceleration for rotation about the ith axis is

$$\ddot{\phi} = \frac{|\mathcal{R}_i \times \mathbf{F}|}{I_i} = \frac{|\mathbf{L}_{q,i} \times (\mathbf{QE})|}{I_i} \tag{1.8}$$

The form of Eq (1.8) suggests that each axis can be assigned a quantity similar to the charge arm,

$$\mathbf{Z}_i = \mathbf{Q}\frac{|\mathbf{L}_{q,i}|}{I_i} = \mathbf{Q}\frac{|\mathbf{L}_q \times \mathbf{R}_i|}{I_i} \tag{1.9}$$

where we have used a mathematical identity to simplify the form of the magnitude of $\mathbf{L}_{q,i}$. We refer to this quantity as the charge lever moment CLM and each ion possesses three CLMs. The CLMs contain detailed information about the distribution of charge and mass in the ion, addressing both the degree to which Coulomb interactions with neighboring ions can induce torque about a given axis through ($|\mathbf{L}_{q,i}|$) and the rate of the dynamic response through I_i. This is considerably more detail than is available from the charge arm and as we show in section 1.2.3 it permits at least limited comparison between ions of different mass.

1.2.3 Interpretation of the model and its limitations

As noted in Sec.1.2.1, the central premise of the CLM model is that the mixing of rapid rotational dynamics with translational motion increases the rate of transport processes. However, the rotational dynamics in liquids are complex, and the CLM model contains many approximations that bear careful consideration.

First, the model relies entirely on rigid body kinematics. In reality, all polyatomic ions possess some degree of vibrational flexibility, creating two problems in the model: (1) the kinematic description will be a poor description of the dynamics of highly flexible ions and (2) the calculation of a single set of CLMs of an ion does not describe the full distribution of conformations present in solution. While many ions will be too flexible to be treated in this formalism, we show in later section that, for relatively rigid ions such as imidazolium species, the values of the CLM are not strongly dependent on the ionic configuration. In

these cases, the CLM calculated from the minimum energy configuration of the isolated ion provides a useful estimate of the values of the configurations accessed in solution. This same robustness in the CLMs ensures that the ion is suitably rigid in the sense that the motion of the ion in response to the applied electric field will not deform the ion to such a degree that it is no longer well described by rigid body kinematics.

There is also evidence from simulation that the alkyl substituents of cations are extended in the liquid state,(Canongia-Lopes & Pádua 2006; Wang & Voth 2006) forming regions of tail aggregation. This implies that the equilibrium geometry in the liquid state includes an extended alkyl chain similar to that of the all-trans configuration of the isolated ion, further supporting the use of the CLMs of the isolated ion as estimators for liquid phase dynamics. Raman spectroscopic studies by Hayashi et al.(Hayashi, Ozawa, & Hamaguchi 2003) imply a significant population of all trans configurations in their studies of 1-butyl-3-methylimidazolium cations, albeit coexisting with a population of cis configurations; a recent review of Raman spectroscopic studies by Berg(Berg 2007) concludes that this is consistent with other studies of similar ions. Thus, while not a perfect model, the isolated ion trans configurations are representative of a large population of ions in the solvent. Another point is that ionic rotation proceeds via a diffusive rather than ballistic mechanism. Interactions with the neighboring ions slow rotation, and the influence of the dynamic effects noted above must be considered carefully. If one views rotation as a series of hops through transition states between local minima, the rate constant for such hopping is given by classical transition state theory(Hänggi, Talkner, & Borkovec 1990)

$$k \approx \frac{\omega_0}{2\pi} \exp[-\beta \Delta G] \tag{1.10}$$

where $\beta = 1/k_b T$, ΔG is the free energy of activation, and ω_0 is the frequency for motion within the metastable well prior to reaction. We anticipate, based on the arguments above,

that ILs composed of ions with large CLMs will sample the configuration space of the liquid more rapidly than those with small CLMs, increasing the frequency ω_0 and thus the rate of rotational diffusion. The changes in ionic structure associated with alteration of the CLM may also affect ΔG but this is apt to be a secondary effect. We have shown in other work(Kobrak 2007; 2008) that ionic volume is the prime determinant of the energy of electrostatic polarization for the liquid, and the distribution of charge within the ion is of secondary importance. Since the transition state energy will be largely determined by the electrostatic polarization energy (for ions incorporating a nonzero CLM), the effect of changes in the CLM (neglecting changes in molar volume) will primarily be to alter the ω_0 prefactor.

Returning to the study of Urahata and Ribeiro noted above,(Urahata & Ribeiro 2005) the significance of the rapid response for rotation about axes orthogonal to the N$-$N axis becomes clearer. The N$-$N axis corresponds roughly to the line from the center of the imidazolium ring along the alkyl substituent (when observed in an all trans configuration). The center of charge sits close to the center of the imidazolium ring, so rotation about this axis does not significantly alter Coulomb interactions with neighboring species. In contrast, libration about axes orthogonal to the N$-$N axis leads to significant displacement of the center of charge, and so couples strongly to the motions of neighboring ions. Thus, these latter librational modes are important contributors to the collective dynamics of the liquid, and their capacity for rapid response to the motion of neighboring ions is consistent with the arguments above.

The next section of this paper is committed to applying the CLM approach to the interpretation of the experimentally observed shear viscosities of ILs. In Sec. 1.3.3, we present the results of calculations of the CLM for a series of ions and show that the calculated values are robust with respect to the ionic geometry. In Sec.1.3.2, we explore the correlation between the shear viscosity of an ionic liquid and the CLM of its component

ions. In Sec.1.3.3, we consider the utility of the CLM approach for the interpretation of Kerr effect spectroscopy in ILs.

1.3 Results and Discussion

1.3.1 Calculation of the CLMs for IL component ions

Application of the theory outlined above requires knowledge of the CLMs of ions used as components in ILs. These are readily obtained from electronic structure calculations analogous to those used in the derivation of force fields for molecular dynamics. The calculations require the optimization of ionic geometry, followed by the fitting of electrostatic charges necessary to determine the center of charge; the latter is carried out via the CHELPG algorithm.(Breneman & Wiberg 1990) Cation and anion calculations were done independently and in isolation (i.e., no dielectric medium or other environment was assumed). Values for the CLMs for all ions are included in Table II.

Electronic structure calculations were carried out using the GAUSSIAN03 software suite,(Frisch *et al.* 2003) making use of density functional theory based on Beckes three−parameter gradient corrected exchange(Becke 1993) and Lee−Yang−Parr gradient-corrected correlation functionals(Lee, Yang, & Parr 1988) (B3LYP) in the 6−31G(d, p) basis set. Atomic charges were calculated via the CHELPG algorithm, which seeks to reproduce the observed electrostatic potential of the molecule or ion by the distribution of charge between atomic sites. A simple FORTRAN program was used to read the output from the GAUSSIAN program and calculate the CLM according to Eq.(1.9).

As noted in early section, there is evidence that alkyl chains are extended in ILs. However, to test the limits of the applicability of the theory, we also examine the robustness of the calculated values of the CLM with respect to non−trans configurations in the alkyl substituents. To this end, we conduct electronic structure calculations in con-

strained geometries to introduce non−trans configurations into the alkyl substituents of three ions: 1−butyl−3−methylimidazolium (C_4MIM^+), 1−octyl−3−methylimidazolium (C_8MIM^+), and N−methyl−N−butylpyrrolidinium ($P14^+$).

Because both (C_4MIM^+) and ($P14^+$) possess a n-butyl substituent, the same scheme was used to generate variant conformations in both cases. For each configuration, we report the maximum CLM (mCLM) of the ion; the motivation for evaluating this function is explained in next section, but for the moment it is sufficient to state that we use the maximum of the three CLMs calculated for each ion as a general indicator of the extent to which the configuration affects the calculated CLMs. Numbering the carbons in the chain from C1 to C4, with C1 being the atom bound to the nitrogen, values of the mCLM were calculated using electronic structure calculations, as described above, with specific dihedral angles constrained to staggered (all-trans), eclipsed, or gauche configurations as indicated in Table I. For completeness, two cases for each ion are reported in which two pairs of dihedral angles are varied simultaneously, and both placed in eclipsed or gauche configurations. The choice of which angles are varied is arbitrary, but the goal is to provide a reasonable measure of the robustness of the mCLM. The results indicate that the mCLM may vary by as much as 50% for C_4MIM^+ and 40% for $P14^+$. While this is significant, the variation in the mCLM for most configurations is significantly smaller. The equilibrium value of the mCLM is thus a reasonable proxy for the ensemble average.

Similar variation was undertaken with the C_8MIM^+ cation, also reported in Table 1.1. The longer chain for C_8MIM^+ would be expected to lead to a significantly greater variation but, in fact, this does not appear to be the case. The largest observed variation was roughly 54%. The greater flexibility of the chain may affect kinematic response, but the introduction of angular disorder does not greatly affect the calculated mCLMs.

Similar studies were undertaken for the BF_4^- and PF_6^- anions to confirm that the mCLM remained small for physically reasonable variation in bond lengths and angles.

This was confirmed, and the details are presented in the supplementary materials for this work. The supplementary materials also include further details on cation configurations, including some sample configurations.

Having ascertained that the CLM values are relatively robust for rigid ions, we now consider their application to interpreting the relative viscosities of ILs.

1.3.2 Correlation between the CLM and the IL viscosity

The CLM formulation assigns three CLMs to each ion. Given that ionic rotation/libration is an important component of the ionic response, some functions of these three CLMs must correlate with viscosity, but the optimal choice of function is by no means clear. However, it is obvious that in a rotationally averaged ensemble of ions, the most rapid response will arise from those ions in which the largest CLM is perpendicular to the direction of the applied electric field. This is consistent with the molecular dynamics simulations of Urahata and Riberiro(Urahata & Ribeiro 2005) noted above, as the rotations orthogonal to the N-N axis (corresponding to larger CLMs) respond much more rapidly than rotations about the N$-$N axis. We therefore anticipate a correlation between the mCLM of an ion and its capacity to respond to a dynamic electric field, and we explore the correlation between the mCLM of an ion and liquid viscosity in ILs.

A second issue is the question of how the CLMs of two component ions should be combined to create a function that correlates with viscosity. We circumvent this challenge by limiting our comparisons to series of ILs in which (1) the identity of one ion (cation or anion) is held constant and (2) the other ion belongs to a structurally homologous series of ions (e.g., dialkylimidazolium ions). This has the additional benefit that well-chosen series of ILs will not possess greatly different capacities for specific interactions such as hydrogen bonding, ensuring that these phenomena do not obscure any correlation with the CLM. This unfortunately places severe restrictions on the available datasets, but we report

Table 1.1. Maximum charge lever moments for three cations, with varying configurations of the dihedral angles in their alkyl substituents. CR indicates a ring carbon, N is the nitrogen to which the substituent is connected, and carbons in the substituent are numbered sequentially with C1 bound to the ring nitrogen. Where multiple bonds are reported, both are constrained to the same configuration (*i.e.* both are eclipsed, or both are gauche).

	Staggered mCLM ($\times 10^{-3}$amu·e/Å)	Eclipsed mCLM ($\times 10^{-3}$amu·e/Å)	Gauche mCLM ($\times 10^{-3}$amu·e/Å)
C_4MIM^+			
CR-NT-C1-C2	1.21	1.68	1.24
NT-C1-C2-C3	1.21	1.38	1.34
C1-C2-C3-C4	1.21	1.20	1.22
NT-C1-C2-C3 and C1-C2-C3-C4	1.21	0.87	1.34
CR-NT-C1-C2 and C1-C2-C3-C4	1.21	1.22	1.22
$P14^+$			
CR-NT-C1-C2	1.26	1.39	1.48
NT-C1-C2-C3	1.26	1.68	1.75
C1-C2-C3-C4	1.26	1.51	1.45
NT-C1-C2-C3 and C1-C2-C3-C4	1.26	0.91	1.52
CR-NT-C1-C2 and C1-C2-C3-C4	1.26	1.38	1.35
C_8MIM^+			
NT-C1-C2-C3	0.93	1.17	1.09
C1-C2-C3-C4	0.93	0.98	1.01
C2-C3-C4-C5	0.93	1.15	1.09
C3-C4-C5-C6	0.93	1.01	1.00
C4-C5-C6-C7	0.93	1.03	1.01
C5-C6-C7-C8	0.93	0.96	0.96
NT-C1-C2-C3 and C1-C2-C3-C4	0.93	1.43	1.12
C4-C5-C6-C7 and C5-C6-C7-C8	0.93	1.06	1.04

three such series that provide ample evidence to support the theory.

Another important issue is that liquid viscosities (and liquid dynamics in general) are strongly temperature dependent. Comparisons between the dynamics of different molecular liquids are best conducted at a common reduced temperature but this is problematic for ILs. ILs decompose chemically before reaching their critical temperature, and the reduced temperature therefore cannot be determined from experimental data. Rather than attempting to formulate some alternative scheme for identifying corresponding states between ILs, we will simply compare structurally homologous ILs at equivalent (room) temperatures and make the assumption that these homologs will have comparable critical temperatures.

The CLMs of 34 ions have been calculated and are reported in Table 1.2. We consider three different sets of ILs presented independently to facilitate the interpretation of the data. The first consists of a series of fluoroborocarbon anions in combination with a common cation, while the latter two sets consist of aromatic and aliphatic cations, respectively, in combination with the bis(trifluoromethylsulfonyl)imide (NTf_2^-) anion.

The datasets for all three studies were chosen based on the availability of experimentally determined viscosities for the ILs in question and the feasibility of accurate electronic structural determination of the CLMs necessary to implement the theory. Chloroaluminate and other coordination complexes were excluded, as these species typically exist in multiple covalent states in solution, complicating the application of the theory. The rigidity and chemically inert character of fluoroborocarbon anions make them an ideal test set for the theory; the cations, particularly the aliphatic species, are less rigid and therefore represent a test of the limits of the CLM approach.

We do not claim that the data presented are comprehensive but they are representative of the literature and the above mentioned issues were the only factors in the selection process. No attempt was made to assess the quality of physical measurements with regard to issues such as sample purity or measurement technique. This adds some uncertainty to

Table 1.2. Charge Lever Moments (CLMs) for some ions commonly used in ionic liquids. anion structures are denoted in chemical notation.

	Ionic Mass (amu)	CLM (a) ($\times 10^{-3}$amu·e/Å)	CLM (b) ($\times 10^{-3}$amu·e/Å)	CLM (c) ($\times 10^{-3}$amu·e/Å)
Aromatic Cations				
C_2MIM^+	111.2	1.43	0.82	0.75
C_4MIM^+	139.2	1.21	1.16	1.05
C_5MIM^+	153.2	1.16	1.08	0.22
C_6MIM^+	167.3	1.10	1.09	0.77
C_8MIM^+	195.3	0.93	0.93	0.68
$C_{10}MIM^+$	223.4	0.78	0.77	0.69
C_3MMIM^+	139.2	0.96	0.79	0.50
C_2MMIM^+	125.2	0.70	0.53	0.45
$IBMIM^+$	139.2	1.25	1.12	1.11
$MNPIM^+$	153.2	1.31	1.20	0.82
$MTMSiMIM^+$	169.3	1.18	1.11	0.67
$Pyr13^+$	136.2	1.11	0.48	0.44
Aliphatic Cations				
$N3111^+$	102.2	1.79	1.76	0.061
$N4111^+$	116.2	1.90	1.87	0.039
$N6111^+$	144.3	1.55	1.53	0.12
$P13^+$	128.2	1.54	0.85	0.67
$P14^+$	142.3	1.26	1.25	1.15
$PP13^+$	142.3	0.90	0.17	0.24
$PIEOM^+$	144.2	1.88	0.43	0.65
Fluorous Anions				
BF_4^-	86.8	0.00	0.00	0.00
$CF_3BF_3^-$	136.8	1.51	1.51	0.00
$C_2F_5BF_3^-$	186.8	1.57	1.48	0.16
$C_3F_7BF_3^-$	236.8	1.52	0.51	0.01
$C_4F_9BF_3^-$	286.8	1.18	1.14	0.21
$CF_3CO_2^-$	113.0	4.81	3.99	0.14
PF_6^-	145.0	0.00	0.00	0.00
$CF_3SO_3^-$	149.1	2.80	2.80	0.00
$C_3F_7CO_2^-$	213.0	2.30	2.30	0.52
$(CF_3SO_2)_2N^-$ (NTf_2^-)	280.1	0.25	0.08	0.00
Non-fluorous Anions				
$CH_3CO_2^-$	75.0	5.6	5.59	0.00
$N(CN)_2^-$	66.0	15.1	0.00	0.89
$CH_3SO_3^-$	96.1	6.97	6.97	0.00
$C_2H_5SO_3^-$	109.1	4.94	4.72	3.08
$C_4H_9SO_3^-$	279.0	1.57	1.48	0.42

Table 1.3. CLM data for fluoroborocarbon anions, and the viscosities of three families of ionic liquids based on fluoroborocarbon anions; see text for details.

Anion	Ionic masses (amu)	mCLM (10^{-3} amu·e/Å)	Viscosity (cP) with counterion: PI1EOM$^+$	OX1EOM$^+$	P1EOM$^+$
BF_4^-	87	0.00	1240	704	213
$CF_3BF_3^-$	136.8	1.51	203	134	87
$C_2F_5BF_3^-$	186.8	1.57	112	90	52
$C_3F_7BF_3^-$	236.8	1.52	131	117	62
$C_4F_9BF_3^-$	286.8	1.18	187	177	84

experimental values and in combination with the theoretical uncertainties described above may be responsible for some of the observed scatter in the trends.

Analysis of the fluoroborocarbons We consider first three families of ILs composed of a common cation in combination with a series of fluoroborocarbon anions, based on experimental data compiled in an extensive survey of these systems by Zhou et al.(Zhou, Matsumoto, & Tatsumi 2006) We choose a set of 15 liquids for study, consisting of five different fluorocarbon anions in combination with three different cations. The three cations were chosen as they were the only ones to produce ILs that were molten at RT for all five of the anions of interest. The cations were N-ethoxymethyl-N-methylpyrrolidinium (P1EOM$^+$), N-ethoxymethyl-N-methylmorpholinium (OX1EOM$^+$) and N-ethoxymethyl-N-methylpiperidinium (PI1EOM$^+$).

We examine the variation in viscosity with the identity of the anion for ILs based on each of these cations. This is a good test of the theory, as the fluorinated anions are chemically inert (i.e., do not engage in hydrogen bonding or other specific interactions), and fluorinated carbon chains are known to be more rigid than their hydrocarbon analogs,(Gomes & Pádua 2003) reducing the potential problems associated with flexibility. The identities of the fluoroborcarbon anions, as well as their calculated mCLM values and viscosities, are given in Table 1.3.

Examination of Fig.1.3 indicates that the viscosity of all three classes of liquids follows the expected trend. As the mCLM increases, the viscosity decreases. The data, and the goodness-of-fit1.6, are heavily biased by the mCLM of BF_4^-, which is zero by symmetry. However, the remainder of the points fall on the expected trend, yielding a remarkably good fit for the available dataset. It is also worth considering that the CLM successfully explains the relatively high viscosity of the ILs based on the BF_4^- ion, which is not easily explained by other means. Its low mass should reduce dispersive interactions, which in a molecular liquid would be expected to lower viscosity. Furthermore, while one might argue that the small radius should increase the magnitude of Coulomb interactions with neighboring ions, this is inconsistent with the observation that the largest ion $C_4F_9BF_3^-$, possesses a viscosity comparable to that of $CF_3BF_3^-$ in all three cases. The latter point is explained in the CLM approach by the counterbalancing effects of an increased distance between the centers of charge and mass and an increase in the moment of inertia for the ion.

The trend is extremely consistent between the three families, including the fact that liquids based on $C_4F_9BF_3^-$ possess lower viscosities than would be expected from the CLM arguments. This deviation could arise from an increase in flexibility associated with the longer chain. Thus, while the dataset is sparse, the CLM approach adequately explains anomalies in the observed viscosities that are not readily explained with reference to other principles.

BF_4^- possesses a much higher viscosity than other fluroborocarbon anions, which makes the data shown in Fig.1.3 too sparse, A modified version of this figure, with BF_4^- dropped, is presented in Fig 1.4. Even without the bias introduced by the BF_4^- anion, the trend remains consistent with the expectations of the theory. The $C_4F_9BF_3^-$ anion falls slightly off the trendline, a phenomenon we attribute to the flexibility of the longer chain; the other ions are remarkably consistent.

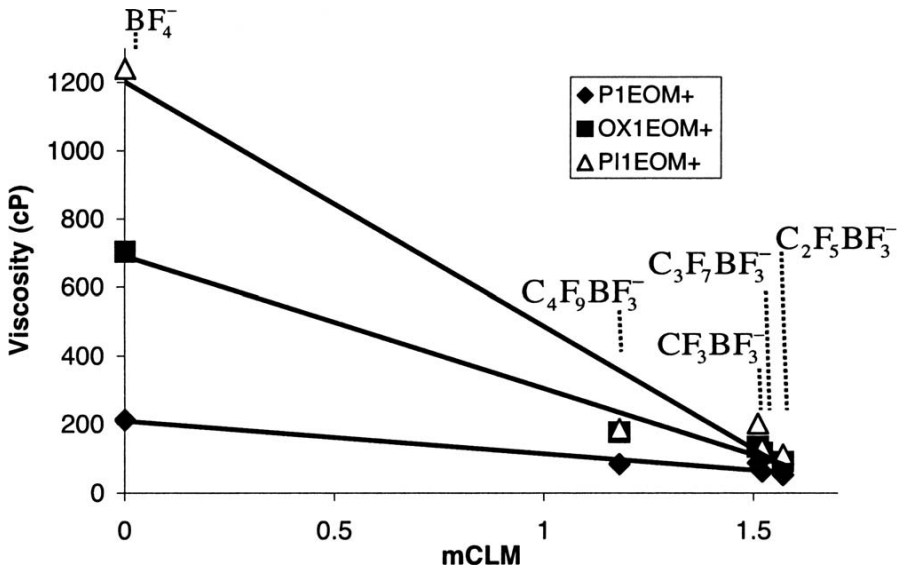

FIG. 1.3. Viscosity vs mCLM for ILs composed of the N−methyl−N−ethoxymethylpiperidinium in combination with fluroborocarbon anions

Analysis of the imidazolium group We examine the viscosities of the 1−alkyl−3−methylimidazolium bis((trifluoromethyl)sulfonyl)imides and related compounds, shown in Fig.1.4. These include those with n−alkyl substituents (C_nMIM^+, with n=2,4,5,6,8,10) and species including methylated C_2−carbons (C_3MMIM^+ and C_2MMIM^+) or branched substituents ($IBMIM^+$ and $MNPIM^+$), as well as one silyl compound ($MTMSiMIM^+$). A plot of viscosity versus mCLM is shown in Fig.1.5, with corresponding data reported in Table 1.4.

The C_nMIM^+ series shows a clear trend: The larger the mCLM, the lower the viscosity, in accordance with the theory. Unlike the fluoroborocarbons discussed above, the trend mimics that which would be expected if increased dispersive interactions were responsible for the differences in viscosity. However, consider that for the C_8MIM^+ to $C_{10}MIM^+$ case, a change in the molar mass of less than 5% produces a viscosity change of almost 22%;

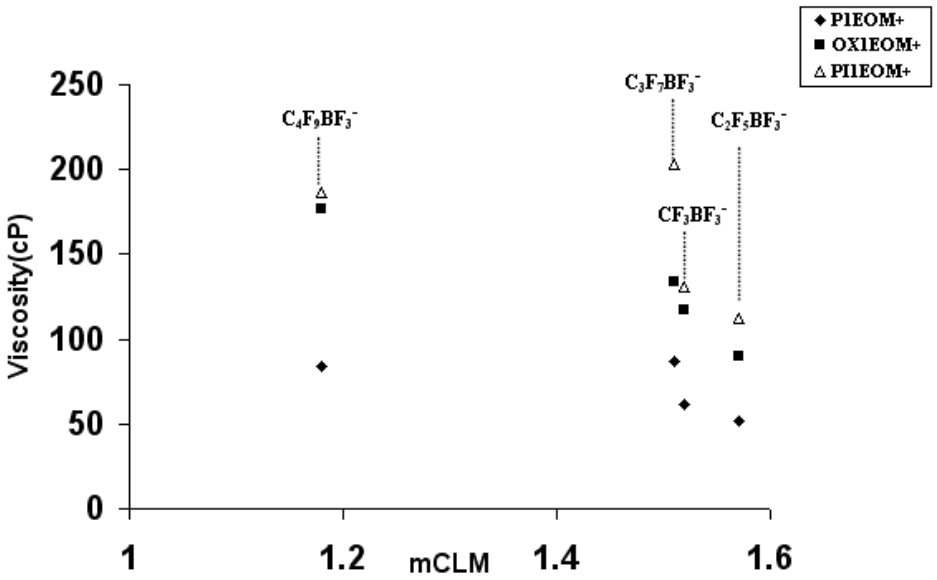

FIG. 1.4. A zoom in picture of Fig.1.3 describing viscosity vs mCLM for ILs composed of the N−methyl−N−ethoxymethylpiperidinium in combination with fluroborocarbon anions except BF_4^-.

this dramatic change cannot be explained with reference to dispersive interactions. The C_3MMIM$^+$ and C_2MMIM$^+$ ions fall near the trendline, a surprising result, as these species are not labile for hydrogen bonding and so might be expected to display disproportionately low viscosities relative to the C_nMIM$^+$ series. This suggests that hydrogen bonding is not a strong determinant of viscosity in these species.

More serious anomalies are observed for species containing branched substituents, including IBMIM$^+$, MNPMIM$^+$, and MTMSiMIM$^+$. Consider that the C_5MIM$^+$ and MNPMIM$^+$ ions have equivalent ionic masses, but the latter viscosity is over three times larger than that of the former. These anomalously high viscosities may arise from the loss

Table 1.4. CLM data for imidazolium cations, and the viscosity of ionic liquids formed in combination with the bis(trifluoromethylsulfonyl)imide anion. Viscosities are experimental, taken from the indicated reference.

Cation	Ionic mass (amu)	mCLM (10^{-3} amu·e/Å)	Viscosity (cP)
C_3MMIM^+	139.2	0.96	90(Valkenburg *et al.* 2005)
C_2MMIM^+	125.2	0.70	88(Matsumoto, Kageyama, & Miyazaki 2002)
$IBMIM^+$	139.2	1.25	83(Hyun *et al.* 2002)
C_2MIM^+	111.2	1.43	25(Hyun *et al.* 2002)
C_4MIM^+	139.2	1.21	44(Hyun *et al.* 2002)
C_5MIM^+	153.2	1.16	50(Hyun *et al.* 2002)
C_6MIM^+	167.3	1.10	59(Hyun *et al.* 2002)
C_8MIM^+	195.3	0.93	74(Hyun *et al.* 2002)
$C_{10}MIM^+$	223.4	0.78	90(Hyun *et al.* 2002)
$MNPIM^+$	153.2	1.31	161(Shirota & Castner 2005b)
$MTMSiMIM^+$	169.3	1.18	98(Shirota & Castner 2005b)

of flexibility in the substituent, which may create friction through interaction with neighboring ions in rotation. That would explain why $MNPMIM^+$ possesses a higher viscosity than its silyl analog, as rotation about the (relatively long) Si−C bond is less strongly hindered. The existence of friction of this type undermines the theory, as it now seems that for the CLM approach to be a good description, the ion must be rigid but not too rigid. Nevertheless, the theory does have significant success in explaining the relative viscosities of the C_nMIM^+ series.

Analysis of the aliphatic group Turning to aliphatic cation species, we consider the ILs of the ions shown in Fig.1.6 in combination with NTf_2^- . (see Table 1.5). Considering first those species based on a ring structure, the theory appears to hold reasonably well. One interesting phenomenon is the increase in the mCLM on the replacement of a substituent carbon with an oxygen ($P14^+$ to $P1EOM^+$), which leads to a dramatic increase in the mCLM and a corresponding decrease in viscosity. As is known from studies on

Table 1.5. CLM data for aliphatic cations, and the viscosity of ionic liquids formed in combination with the bis(trifluoromethylsulfonyl)imide anion. Viscosities are experimental, taken from the indicated reference.

Cation	Ionic masses (amu)	mCLM (10^{-3} amu·e/Å)	Viscosity (cP)
$N3111^+$	102.2	1.79	72(Hajime, Hikari, & Kuniaki 2005)
$N4111^+$	116.2	1.90	132(Tokuda *et al.* 2006)
$N6111^+$	144.3	1.55	153(Sun, Forsyth, & MacFarlane 1998)
$P13^+$	128.2	1.54	63(MacFarlane *et al.* 1999)
$P14^+$	142.3	1.26	85(Shirota *et al.* 2005)
$PIEOM^+$	144.2	1.88	68(Shirota *et al.* 2005)
$PP13^+$	142.3	0.90	151(Hajime, Hikari, & Kuniaki 2005)

polyethylene oxide,(Engkvist & Karlström 1997) the presence of the oxygen introduces an out-of-plane bend into the substituent (see Fig.1.7). This changes the moment of inertia, and by the arguments above must alter the dynamics. The reduction in IL viscosity with the inclusion of ethoxy-substituents is well known and is readily interpreted within the present theory.

The acyclic aliphatics behave more oddly. The N3111 ion appears to fall in line with the cyclic aliphatics, but the N4111 and N6111 ions do not obey the trend. It is also odd that while the ionic mass of N4111 is only 15% higher than that of N3111, its viscosity is twice as high. This seems inconsistent with the observation that a 24% difference in mass between N4111 and N6111 leads to only a 16% increase in viscosity. These discrepancies likely arise from the breakdown in the assumption of a rigid ion, on which the CLM is based. The longest chain in the N3111 is five heavy atoms (including one methyl, one nitrogen atom, and the propyl group), while that for N4111 is six atoms. Why this should lead to such an abrupt change in behavior is unclear, but it does seem related to the increasing flexibility of the ion.

Parameters for the regression analysis of Fig.1.8 (including only the cyclic cations) are reported in Table 1.6. Comparing the reported values for the aliphatic and aromatic

Table 1.6. Regression parameters for viscosity vs. mCLM data shown in Figures 1.3,1.6 and 1.9.

	Slope (10^{-3} cP·Å/e)	Intercept (cP)	R^2
Fluoroborocarbons			
PI1EOM$^+$	-715.2	1201.3	0.959
OX1EOM$^+$	-386.3	691.0	0.983
P1EOM$^+$	-95.87	210.4	0.958
Imidazolium	-96.5	164.7	0.898
Aliphatic	-88.6	211.9	0.778

species, we note that their slopes agree to within 11% and their intercepts to within 30%. This agreement is remarkable and likely arises from the fact that both classes of liquids in this study were formed by combination with the same anion, and that the cyclic aliphatics possess at least a superficial structural similarity to the aromatics (i.e., both groups contain five-membered rings decorated with alkyl substituents). The agreement is remarkable and provides further validation of the CLM approach.

1.3.3 Kerr Effect Spectroscopy

As noted above, the decision to focus on the analysis of the shear viscosity is driven both by the large quantity of the available experimental data and the importance of viscosity as a determinant of the utility of ILs in applications. However, the CLM approach is a general framework for understanding liquid dynamics and so can be applied to the interpretation of other properties.

We compare the CLM data with experimentally observed Kerr effect spectra for ILs. Optical heterodyne-detected Raman-induced Kerr effect spectroscopy (OHD-RIKES), which is a nonlinear optical polarization technique, can measure the time derivative of the polarizability-polarizability correlation function for transparent condensed phase sample (Deeg *et al.* 1989; Ruhman *et al.* 1987). The working mechanism of OHD-RIKES consists of two

linearly polarized optical pulses, with a time delay between them. The pulses interact non-resonantly with the isotropic sample, and the birefringence induced by the first pulse will alter the interaction of the medium with the second pulse; the decay of the birefringence therefore provides insight on the dynamics of the system. Because of its broad range of time scales (ranging from 20 fs to 1 ns) and high signal to noise ratio, OHD-RIKES is widely used as a tool to investigate the intermolecular dynamics and relationship between dynamics and local structure in condensed phases (Xiao *et al.* 2006; Giraud *et al.* 2003).

Kerr effect spectroscopy provides perhaps the most detailed description of ionic dynamics in the neat liquid, and while the available dataset is far less extensive than that for viscosity, it is worthy of discussion. A number of studies of Kerr effect spectroscopy in ionic liquids have been reported,(Shirota *et al.* 2005; Giraud *et al.* 2003; Hyun *et al.* 2002; Xiao *et al.* 2006) and these studies are typically comparative across a range of several ILs of some structural similarity. It is therefore possible to make comparisons similar to those for viscosity, albeit on a far more limited dataset. To simplify the discussion, we consider only those studies for which time-domain data are reported, as the comparison of time and frequency domain data, fit to different functional forms, would significantly complicate the discussion.

$$S(t) = \sum_{i=1}^{N} A_i \exp^{-t/\tau_i} \tag{1.11}$$

The available time-domain data are presented as biexponential and triexponential fits shown as equation 1.11 and summarized in Table 1.7. The fitting parameter A and relaxation time τ for different time domain have been listed. The Hyun et al.(Hyun *et al.* 2002) considered the Kerr effect spectra of a series of ILs liquids [C_nMIM$^+$][NTf_2^-], for n=2,4,6,8,10and fitted time-domain spectra based on data between 0.5 and 8 ps. The results show that the response is dominated by a subpicosecond component with a small contri-

bution from a component with a response of the order of 10 ps. Comparing the trend in the time constant for the subpicosecond response with the mCLM values for the cations, we find that, in fact, the ions follow the reverse trend with the rate of the response increasing with increasing mCLM. This is unsurprising in light of the results of Urahata and Ribeiro(Urahata & Ribeiro 2005) discussed above, which indicate a 30-100 ps time scale for the librational response, far too long to contribute to the subpicosecond dynamics. Other simulation studies(Kobrak 2006; 2007) have shown that the subpicosecond solvation dynamics of IL solutions are dominated by the translational response of ions rather than rovibrational response, consistent with the inference for the neat liquid drawn above. The observed Kerr effect data therefore reflect some aspect of translational behavior, and the present study offers no insight on it. The short-time data reported by Xiao et al., comparing the response of $[C_5MIM^+][NTf_2^-]$ and $[C_5MIM^+][Br^-]$ consider only 6 ps of data, and therefore cannot be analyzed in the CLM approach.

Shirota et al.(Shirota *et al.* 2005) reported fitting of the time-domain data on time scales of up to 740 ps, including a short-time window (12 ps) that is sampled with high precision and a longtime window (740 ps) sampled more sparsely. There is significant uncertainty in the fitting of the long-time components, and the interested reader should examine their paper for a discussion of this point. However, the estimation of the long-time scale response permits us to test whether the CLM theory facilitates interpretation of the Kerr effect data on the time scale of the librational response. Comparing first $[P14^+][NTf_2^-]$ and $[P1EOM^+][NTf_2^-]$, it is clear that the higher mCLM of P1EOM+ is associated with a significant reduction in the time constant of the long-time response. Considering next the liquids based on a common cation in combination with Br^-, NTf_2^-, and $N(CN)_2^-$., the bromide responds on a far longer time scale than either of the other two liquids (though the relative error associated with the Br^- measurement is also larger). The more rapid relaxation of NTf_2^-. relative to $N(CN)_2^-$. may arise from the vibrational flexibility of NTf_2^-,

Table 1.7. Summary of experimental Kerr effect data for some ionic liquids.

Liquid	Functional Form	A_1	τ_1 (ps)	A_2	τ_2 (ps)	A_3	τ_3 (ps)
Hyun *et al.*(Hyun *et al.* 2002)							
C_2MIM^+ NTf_2^-	Biexponential	0.030	0.47	0.006	12.6	-	-
C_4MIM^+ NTf_2^-	Biexponential	0.020	0.50	0.002	8.98	-	-
C_5MIM^+ NTf_2^-	Biexponential	0.049	0.30	0.001	8.8	-	-
C_6MIM^+ NTf_2^-	Biexponential	0.042	0.29	0.003	8.5	-	-
C_8MIM^+ NTf_2^-	Biexponential	0.050	0.20	0.003	8.4	-	-
Xiao *et al.*(Xiao *et al.* 2006)							
C_5MIM^+ NTf_2^-	Biexponential	0.8811	0.115	0.0915	2.62	-	-
C_5MIM^+ Br^-	Biexponential	0.9200	0.12	0.0716	0.67	-	-
Shirota *et al.*(Shirota *et al.* 2005)							
$P14^+$ NTf_2^-	Triexponential	0.72	2.43	0.22	18.3	0.06	253
$P1EOM^+$ NTf_2^-	Triexponential	0.68	2.27	0.26	14.6	0.06	161
$P1EOE^{+*}$ NTf_2^-	Triexponential	0.71	2.31	0.23	15.4	0.06	165
$P1EOE^+$ Br^-	Triexponential	0.78	1.89	0.17	21.2	0.05	3200
$P1EOE^+$ $N(CN)_2^-$	Triexponential	0.78	2.02	0.20	16.2	0.02	686
Cang *et al.*(Cang, Li, & Fayer 2003)							
C_2MIM^+ NO_3^-	Mode Coupling Theory	-	-	-	-	-	790
Li *et al.*(Li *et al.* 2006)							
$Pyr13^+$ NTf_2^-	Mode Coupling Theory	-	-	-	-	-	830

*$P1EOE^+$ denotes the *N*-ethoxyethyl-*N*-methylpyrrolidinium cation, similar to $P1EOM^+$ presented in Figure 1.9.

which we have noted elsewhere.(Kobrak & Sandalow 2006; Kobrak 2007) Thus, while the dataset is small, it does appear possible to interpret the long-time scale responses of the IL with reference to the CLM theory.

The results of two additional studies including long-time Kerr response data by Fayer et al.(Li *et al.* 2006; Cang, Li, & Fayer 2003) are presented in Table 1.7. The authors presented temperature-dependent data, though we include data only for liquids at 295 K, which are close to the (RT) values for the other liquids. They use a functional form based on mode coupling theory to analyze their data; the functional forms in the short- and intermediate-time regimes are quite complex and not easily comparable to those used in the other studies discussed here. However, the long-time component of the decay is exponential and so can be directly compared to that in other studies.

The first liquid, $[C_2MIM^+][NO_3^-]$, actually melts at 313 K and so the parameters reported here are for the supercooled liquid. Unfortunately, without long-time data for a comparable liquid (e.g., one based on the C_2MIM^+ cation), we cannot make a meaningful comparison with other liquids. We report the value for completeness. In the case of $[Pyr13^+][NTf_2^-]$, however, we can make direct comparison to other liquids based on the NTf_2^-. anion. The dynamics of the $Pyr13^+$ species are significantly slower than those for the liquids reported by Castner, consistent with the relatively low mCLM of $Pyr13^+$.

1.4 Conclusion

We have investigated the relationship between the viscosity of ILs and the structure of their component ions. We have defined a new property termed the CLM, which serves as a descriptor for the magnitude of the coupling between librational and translational ionic motion. For purposes of this paper we have assumed that the largest CLM (termed the mCLM) can be used as an estimator for this coupling, though we have made no attempt to

find an optimal descriptor based on an ion's three CLMs. It has been shown that the mCLM can be used to interpret the relative viscosities of structurally analogous ILs. The correlation breaks down for highly flexible ions, as expected based on the assumptions used in its derivation, but is useful for a wide range of ions. Analysis of the Kerr effect spectroscopic data implies that the rotational dynamics of ions are relevant to the slowest components of the response, consistent with earlier theoretical studies of solvation dynamics.

The similarity in the fitted parameters describing the variation in the viscosity with mCLM between ILs based on aliphatic and aromatic cations implies that despite its limitations, the theory is relatively robust. Certain structural features of ions, such as the branching of alkyl substituents, appear to have significant effects on viscosity that are not properly accounted for by the theory. These are issues that may benefit from further study.

The two phenomena considered here, shear viscosity and Kerr effect spectroscopy, were chosen because the availability of experimental data made a comparative study possible. The connection between the CLM and the dynamics of the liquid means that it should be relevant in addressing any phenomenon involving a dynamic liquid response to an applied electric field. An obvious extension would be application to properties such as conductivity and ionic diffusion, where the applied electric field is generated by the translation of charge carriers. Another important application would be in chemical kinetics, where any reaction involving the redistribution of charge is electrostatically coupled to the medium. This is best understood in the context of Marcus theory for charge transfer reactions, but any rearrangement of electronic charge that changes the dipole moment of the reactive complex is coupled to the dynamics of the medium. Thus, the CLM approach may be valuable in interpreting the results of a host of different classes of experiments.

While the limited analysis here is sufficient to establish the CLM as a parameter that is relevant to the transport properties of ILs, many questions remain unanswered. The highly ordered structure of ILs, both with respect to their charge ordering and the evidence of

nanoscale organization discussed in Sec. II C, will certainly influence transport properties. Indeed, simulations by Hu and Margulis,(Hu & Margulis 2007) indicate that the dynamic response of an IL depends strongly on the length scale over which it is applied, suggestive of very complex dynamics. The CLM approach is useful as a means of understanding how rotational and translational motions are coupled in ILs, and may serve as the basis for useful descriptors in future QSPR studies. However, the collective dynamics of the liquid and the influence of electrostatic coupling on transport properties in ILs remain areas in need of further investigation.

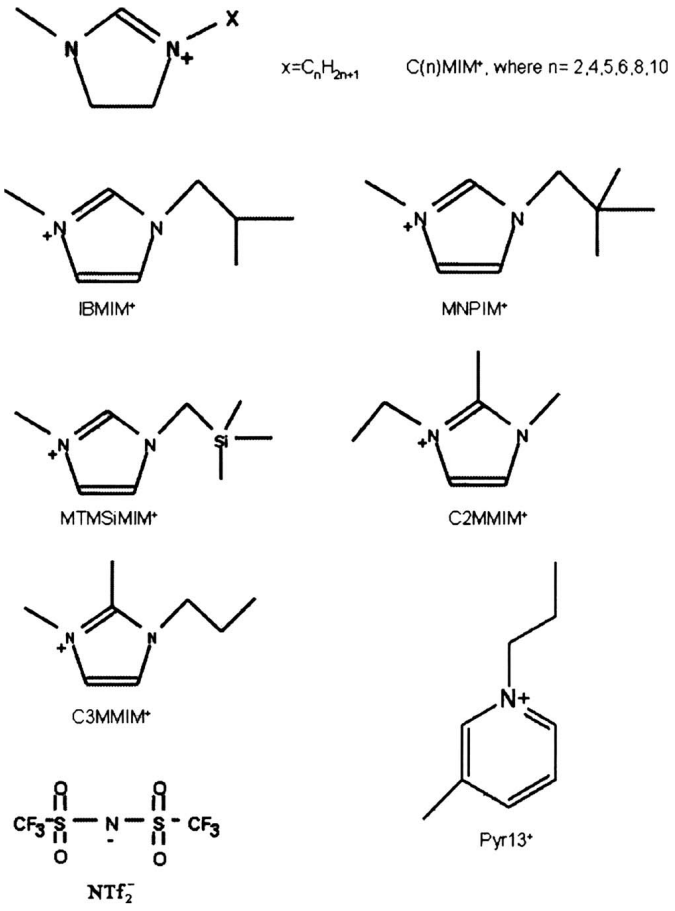

FIG. 1.5. Structures of ions used in studies of aromatic species.

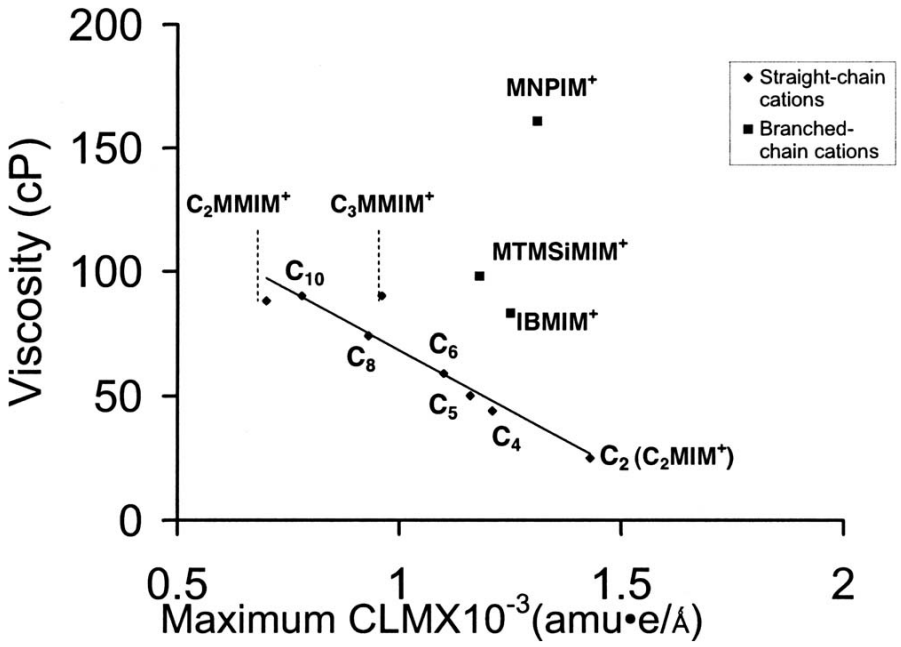

FIG. 1.6. Viscosity vs mCLM for ILs composed of various imidazoliumbased cations in combination with NTf_2^- .

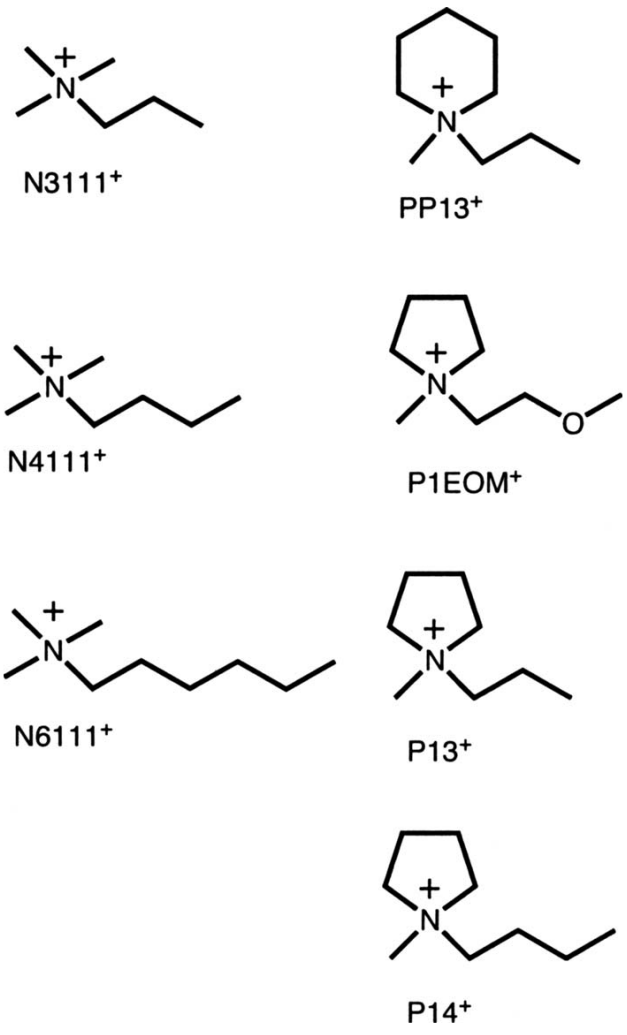

FIG. 1.7. Structures of ions used in studies of aliphatic species.

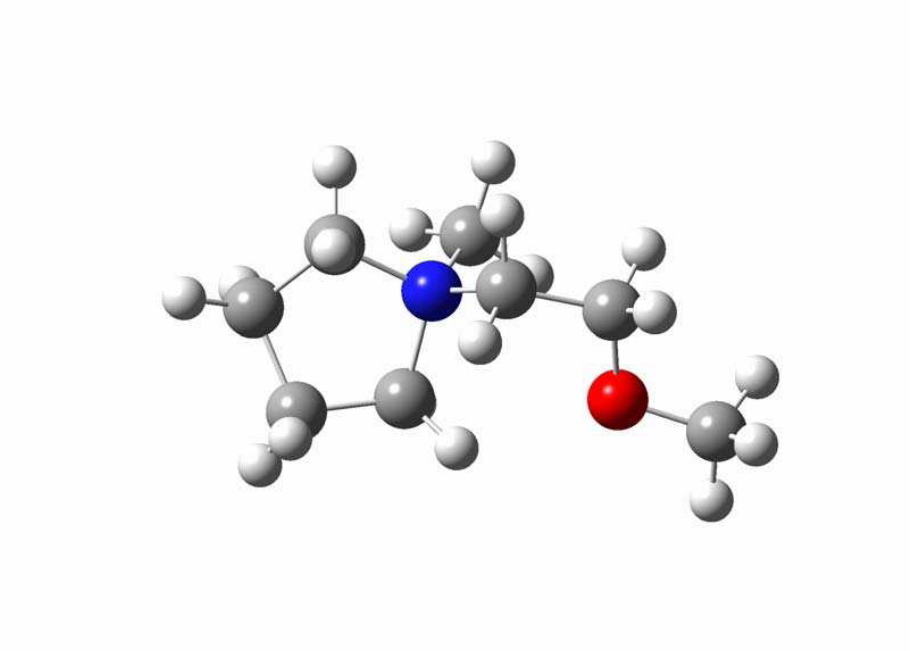

FIG. 1.8. Three-dimensional structure of $P1EOM^+$

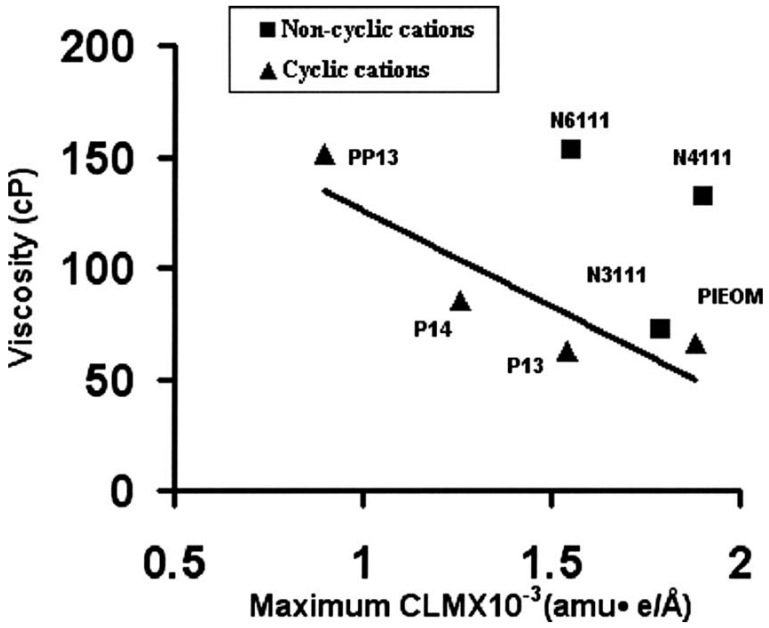

FIG. 1.9. Viscosity vs mCLM for ILs composed of various aliphatic cations in combination with NTf_2^-

Appendix

Part I: Graphical and coordinate representations of representative cations described in Chapter 1.

Newman projections of the staggered, eclipsed and gauche conformation of $P14^{+}$ on the dihedral C1-C2-C3-C4:

Gauche:

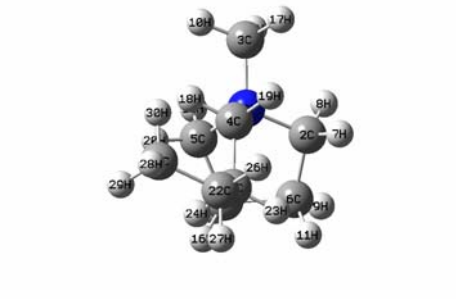

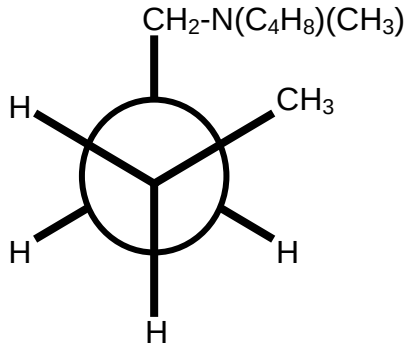

Eclipsed:

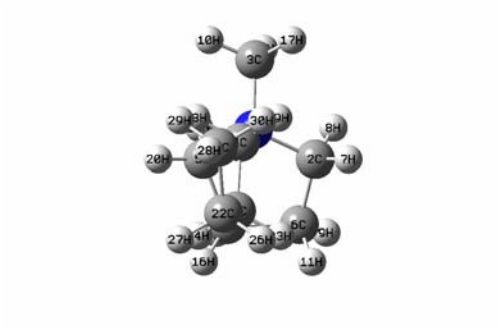

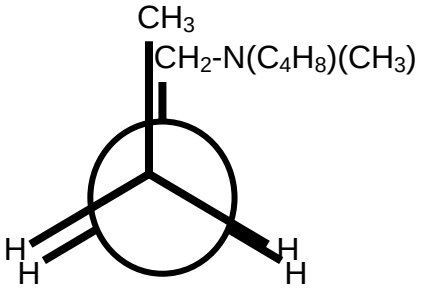

Staggered:

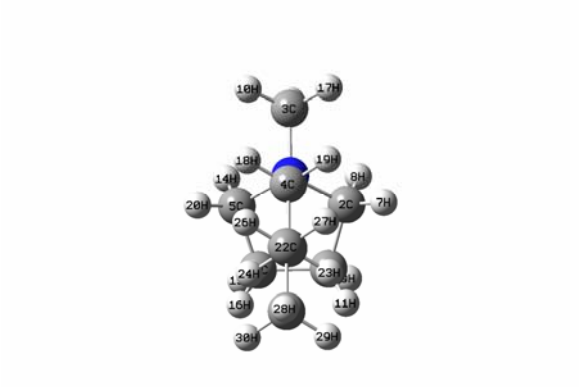

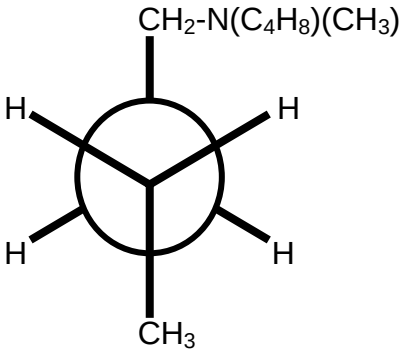

C_4MIM^+ (Eclipsed conformation on dihedral CR-NT-C1-C2, numbered as 9C-11N-4C-14C)

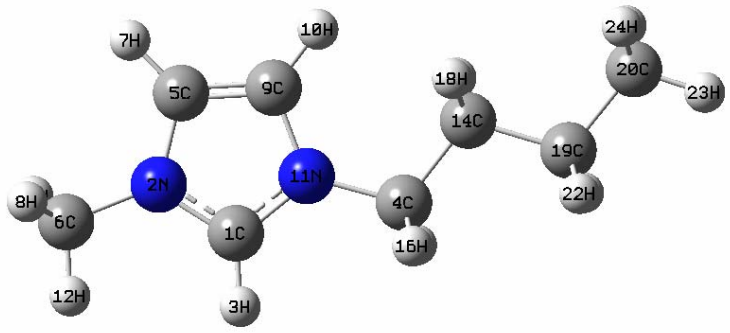

Center Number	Atomic Number	Atomic Type	Coordinates (Angstroms) X	Y	Z
1	6	0	1.657937	-0.892809	-0.007738
2	7	0	2.652573	0.004051	0.013443
3	1	0	1.781245	-1.964780	-0.006090
4	6	0	-0.853205	-0.877019	-0.024530
5	6	0	2.097441	1.270197	-0.001354
6	6	0	4.089547	-0.303302	0.034406
7	1	0	2.704152	2.161966	0.005139
8	1	0	4.560591	0.092339	-0.866919
9	6	0	0.743260	1.113317	-0.030786
10	1	0	-0.048396	1.845276	-0.052331
11	7	0	0.487852	-0.245207	-0.036876
12	1	0	4.220682	-1.384365	0.067724
13	1	0	4.543592	0.144266	0.919839
14	6	0	-1.989087	0.149737	-0.003425
15	1	0	-0.887880	-1.525371	0.854591
16	1	0	-0.909469	-1.518137	-0.908423
17	1	0	-1.879939	0.791196	0.879829
18	1	0	-1.908207	0.802740	-0.881409
19	6	0	-3.364993	-0.533086	0.009006
20	6	0	-4.517229	0.475548	0.030191
21	1	0	-3.435431	-1.192050	0.884021
22	1	0	-3.457397	-1.179765	-0.873056
23	1	0	-5.481412	-0.039066	0.041176
24	1	0	-4.495852	1.123186	-0.852419
25	1	0	-4.471285	1.115153	0.917745

C_4MIM^+ (Gauche conformation on both dihedrals NT-C1-C2-C3 and C1-C2-C3-C4)

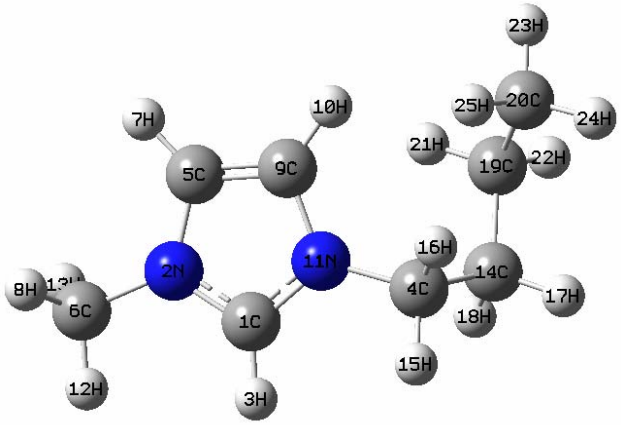

Center Number	Atomic Number	Atomic Type	Coordinates (Angstroms) X	Y	Z
1	6	0	-1.378772	0.901857	-0.154057
2	7	0	-2.249217	-0.092293	0.065251
3	1	0	-1.610170	1.955293	-0.121553
4	6	0	1.063895	1.144731	-0.683920
5	6	0	-1.579912	-1.294545	-0.069427
6	6	0	-3.675778	0.065595	0.381156
7	1	0	-2.076260	-2.243882	0.056229
8	1	0	-4.276826	-0.390990	-0.406925
9	6	0	-0.284045	-0.999407	-0.374235
10	1	0	0.558464	-1.646114	-0.561040
11	7	0	-0.178223	0.377932	-0.425208
12	1	0	-3.909287	1.127779	0.446308
13	1	0	-3.890625	-0.412039	1.338324
14	6	0	2.020154	1.140120	0.512094
15	1	0	0.758174	2.161322	-0.943718
16	1	0	1.529095	0.704597	-1.570112
17	1	0	2.901444	1.747904	0.272417
18	1	0	1.532084	1.614885	1.372440
19	6	0	2.450374	-0.286970	0.883371
20	6	0	3.172162	-0.996834	-0.265783
21	1	0	1.566729	-0.867401	1.178526
22	1	0	3.104923	-0.251426	1.763751
23	1	0	3.463195	-2.008879	0.026898
24	1	0	4.081183	-0.460370	-0.556951
25	1	0	2.531487	-1.077442	-1.150088

$P14^{+}$ (Eclipsed conformation on dihedral NT-C1-C2-C3)

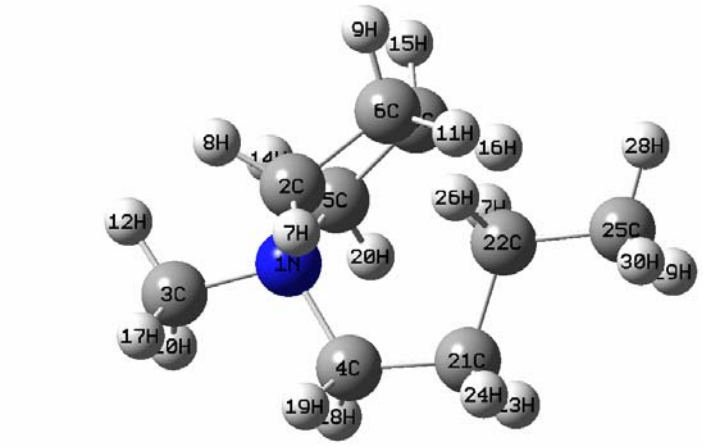

Center Number	Atomic Number	Atomic Type	Coordinates (Angstroms) X	Y	Z
1	7	0	-1.260716	0.192888	0.000018
2	6	0	-0.854244	-0.653990	-1.208172
3	6	0	-2.749997	0.421554	0.000282
4	6	0	-0.599205	1.577395	-0.000967
5	6	0	-0.853791	-0.653002	1.208582
6	6	0	0.346187	-1.508131	-0.775803
7	1	0	-0.663574	0.013475	-2.049819
8	1	0	-1.718098	-1.275368	-1.450374
9	1	0	0.241441	-2.517326	-1.178707
10	1	0	-3.024107	0.985157	0.892592
11	1	0	1.280926	-1.103716	-1.166288
12	1	0	-3.259351	-0.541944	-0.000047
13	6	0	0.349277	-1.503435	0.777266
14	1	0	-1.716265	-1.276998	1.449131
15	1	0	0.251624	-2.510573	1.187044
16	1	0	1.283248	-1.091398	1.161499
17	1	0	-3.024298	0.985865	-0.891519
18	1	0	-0.997928	2.084148	0.882267
19	1	0	-0.997520	2.082433	-0.885376
20	1	0	-0.666199	0.014669	2.050783
21	6	0	0.924241	1.640423	-0.000611
22	6	0	1.508735	0.214194	0.000742
23	1	0	1.292479	2.173325	0.882427
24	1	0	1.292613	2.171574	-0.884607
25	6	0	3.039877	0.213236	-0.001058
26	1	0	1.138700	-0.330685	-0.876961
27	1	0	1.140684	-0.328145	0.880836
28	1	0	3.423962	-0.809905	0.000092
29	1	0	3.441167	0.719257	0.883212
30	1	0	3.439034	0.716474	-0.887871

$P14^{+}$ (Gauche conformation on both dihedrals NT-C1-C2-C3 and C1-C2-C3-C4)

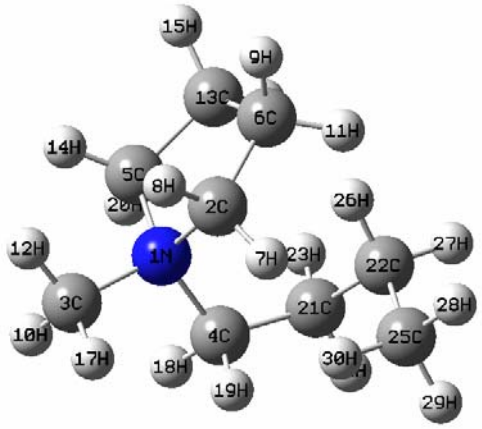

Center Number	Atomic Number	Atomic Type	Coordinates (Angstroms) X	Y	Z
1	7	0	0.919201	-0.613492	-0.077222
2	6	0	0.413038	0.219695	-1.256943
3	6	0	1.781339	-1.746721	-0.569924
4	6	0	-0.221892	-1.243593	0.732308
5	6	0	1.754151	0.368083	0.748075
6	6	0	0.299815	1.670641	-0.767583
7	1	0	-0.519877	-0.218447	-1.614620
8	1	0	1.162980	0.122517	-2.043810
9	1	0	0.659458	2.348085	-1.544439
10	1	0	2.169560	-2.298096	0.286972
11	1	0	-0.737389	1.939964	-0.564013
12	1	0	2.607074	-1.339835	-1.153340
13	6	0	1.157739	1.764703	0.523608
14	1	0	2.772571	0.303522	0.361099
15	1	0	1.962917	2.495198	0.424387
16	1	0	0.547320	2.075433	1.372458
17	1	0	1.178689	-2.408643	-1.192556
18	1	0	0.272150	-1.831900	1.510574
19	1	0	-0.708345	-1.940152	0.043782
20	1	0	1.758118	0.031508	1.785852
21	6	0	-1.255295	-0.310847	1.354339
22	6	0	-1.957745	0.504851	0.251177
23	1	0	-0.781978	0.382038	2.058058
24	1	0	-2.010427	-0.879181	1.907549
25	6	0	-2.682070	-0.387854	-0.760174
26	1	0	-1.217077	1.125415	-0.268911
27	1	0	-2.674149	1.196799	0.711755
28	1	0	-3.169452	0.217862	-1.528227
29	1	0	-3.454553	-0.994863	-0.276609
30	1	0	-1.986472	-1.066527	-1.264712

C_8MIM^+ (Eclipsed conformation on dihedral NT-C1-C2-C3)

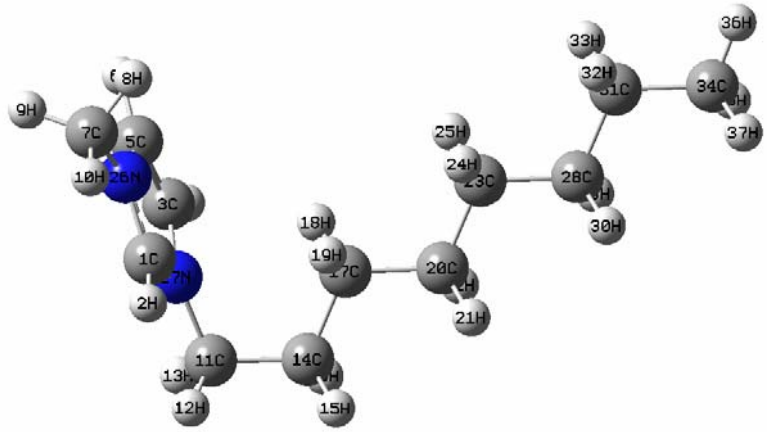

Center Number	Atomic Number	Atomic Type	Coordinates (Angstroms) X	Y	Z
1	6	0	-3.066315	-0.156439	-0.740765
2	1	0	-3.304592	0.060376	-1.770622
3	6	0	-2.409456	0.067311	1.351749
4	1	0	-2.028104	0.570873	2.225741
5	6	0	-2.807263	-1.224708	1.173155
6	1	0	-2.839456	-2.054489	1.861448
7	6	0	-3.730663	-2.568434	-0.773507
8	1	0	-2.971643	-3.350871	-0.725639
9	1	0	-4.634228	-2.892957	-0.254943
10	1	0	-3.967326	-2.356730	-1.815718
11	6	0	-2.235786	2.134457	-0.134719
12	1	0	-2.757443	2.408537	-1.055095
13	1	0	-2.662509	2.731523	0.675665
14	6	0	-0.726627	2.359449	-0.263167
15	1	0	-0.502376	2.781833	-1.250596
16	1	0	-0.408948	3.102137	0.479053
17	6	0	0.054852	1.051916	-0.067489
18	1	0	-0.182874	0.629799	0.918442
19	1	0	-0.279252	0.312562	-0.807934
20	6	0	1.572777	1.243648	-0.187160
21	1	0	1.808283	1.667144	-1.173238
22	1	0	1.903630	1.986159	0.552033
23	6	0	2.360320	-0.057782	0.010332
24	1	0	2.027037	-0.799252	-0.729168
25	1	0	2.119200	-0.480859	0.995537
26	7	0	-3.214619	-1.345719	-0.142492
27	7	0	-2.581381	0.719973	0.145641
28	6	0	3.878322	0.127609	-0.105012
29	1	0	4.210968	0.871120	0.633164
30	1	0	4.119635	0.549775	-1.090834
31	6	0	4.667393	-1.172423	0.095638

32	1	0	4.333487	-1.914886	-0.641604
33	1	0	4.425355	-1.592895	1.080970
34	6	0	6.182149	-0.980936	-0.021271
35	1	0	6.551356	-0.269572	0.725877
36	1	0	6.714878	-1.924888	0.127950
37	1	0	6.458701	-0.596216	-1.009232

C_8MIM^+ (Gauche conformation on both dihedrals NT-C1-C2-C3 and C1-C2-C3-C4)

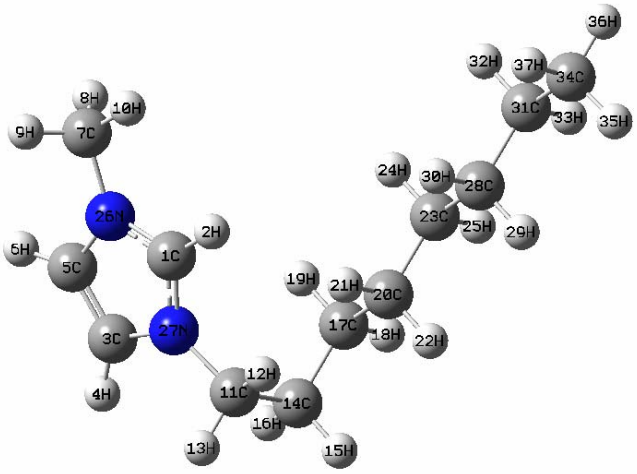

Center Number	Atomic Number	Atomic Type	Coordinates (Angstroms) X	Y	Z
1	6	0	1.831630	0.764227	-0.598861
2	1	0	0.911299	1.033138	-1.093902
3	6	0	3.514890	-0.410925	0.204755
4	1	0	4.102556	-1.290101	0.415861
5	6	0	3.732475	0.899057	0.514696
6	1	0	4.544362	1.373575	1.042894
7	6	0	2.491203	3.074794	0.098558
8	1	0	2.446658	3.368463	1.148502
9	1	0	3.325594	3.576530	-0.394096
10	1	0	1.559921	3.351330	-0.394669
11	6	0	1.673710	-1.710725	-0.992500
12	1	0	0.934394	-1.398816	-1.734431
13	1	0	2.443252	-2.284496	-1.515849
14	6	0	1.026038	-2.530668	0.126828
15	1	0	0.588233	-3.443977	-0.294960
16	1	0	1.801194	-2.848352	0.835070
17	6	0	-0.057416	-1.724858	0.858565
18	1	0	-0.473718	-2.331526	1.674287
19	1	0	0.398930	-0.844563	1.331174
20	6	0	-1.191950	-1.273961	-0.071329
21	1	0	-0.773390	-0.668614	-0.887126
22	1	0	-1.644164	-2.156011	-0.545333
23	6	0	-2.279701	-0.471067	0.653314
24	1	0	-1.825063	0.409909	1.127554
25	1	0	-2.693101	-1.077679	1.471167
26	7	0	2.668446	1.619070	0.003879
27	7	0	2.323865	-0.474960	-0.493516
28	6	0	-3.418158	-0.020020	-0.269982
29	1	0	-3.872700	-0.901477	-0.744102
30	1	0	-3.004537	0.585543	-1.088831
31	6	0	-4.506703	0.783026	0.453317

32	1	0	-4.051328	1.662795	0.927565
33	1	0	-4.919036	0.176687	1.270991
34	6	0	-5.640111	1.230930	-0.473824
35	1	0	-6.137599	0.371429	-0.936799
36	1	0	-6.399302	1.798994	0.072109
37	1	0	-5.264081	1.869590	-1.280838

Part II: Analysis of the robustness of the mCLM values of tetrafluoroborate and hexafluorophosphate anions.

The tables below contain representative information on how variation in chemical structure affects the mCLM, and the energy (in multiples of kT) associated with a given distortion.

BF_4^-		
Variation of the F-B-F bond angle	mCLM ($x10^{-3}$ amu e/Å)	Energy (x kT, T=298K)
109.5^o	0.00	1(equil)
105^o	0.26	14
Variation of the B-F bondlength		
1.41	0.00	1 (equil)
1.47	0.47	1.8
1.5	1.14	3.1

PF_6^-		
Variation of the F-P-F bond angle	mCLM ($x10^{-3}$ amu e/Å)	Energy (x kT, T=298K)
90^o	0.00	1 (equil)
85^o	0.17	8.5
Variation of the P-F bondlength		
1.64	0.00	1 (equil)
1.70	0.08	7.7

For hexafluorophosphate, even unphysically large changes in bond angle and bondlength do not lead to significant changes in mCLM. For tetrafluoroborate, mCLM is largely invariant with respect to bond angle, but some variation in the mCLM is observable for bond stretches within thermally accessible energies. However, these energies are sufficiently high that the ensemble-averaged mCLM will remain negligible.

Chapter 2

A MOLECULAR DYNAMICS STUDY OF THE INFLUENCE OF IONIC CHARGE DISTRIBUTION ON THE DYNAMICS OF A MOLTEN SALT

abstract The distribution of charge in an ion of a fused salt is known to be an important determinant of liquid dynamics. However, the details of this relationship remain poorly understood. We present the results of molecular dynamics simulations on a model molten salt system and show that changes in the distribution of ionic charge can have a profound effect on liquid dynamics. In particular, we observe complex relationships between the distribution of charge, the rate of ionic rotation, and the translational diffusion of ions in the liquid.

2.1 Introduction

In this chapter, we build on the insights obtained in the previous chapter by conducting a series of molecular dynamics (MD) simulations on ILs composed of rigid model ions. The model ions possess a high (octahedral) symmetry in their mass distribution, and the distribution of charge is varied to incorporate both symmetric and asymmetric distributions. Both the structure and the dynamics of the liquids are studied to determine how variation in

the charge distribution of the ions influences liquid behavior. We find that the introduction of asymmetry to the charge distribution has a profound effect on liquid dynamics.

This work is similar in spirit to a study by Chelli et al.,(Chelli, Cardini, & Califano 1997) who performed MD simulations to analyze translational rotational coupling in a NaCN plastic crystal. They interpreted their results with reference to earlier work in a similar vein.(Lynden-Bell, McDonald, & Klein 1983) Chelli et al. considered a crystalline system, making it possible for the authors to directly connect the rotational dynamics of the CN^{-}. ion to the local modes of the surrounding Na^{+} cations, confirming a strong coupling of rotational and translational dynamics for an asymmetric ion in a salt environment. The authors also demonstrated that the rotational motions are incorporated in larger collective motions of the crystal. While we do not directly address this question in the present study, we will return to the issue of collective motion in the Sec. 2.4 of this chapter.

It must be noted that certain phenomena characteristic of real ILs are not explored in the present study. Wang and Voth(Wang & Voth 2006) and Lopes and Pádua(Canongia-Lopes & Pádua 2006) have used MD simulation to show that the aliphatic substituents of ILs aggregate in solution, and they infer that such structural inhomogeneity may influence dynamics in complex ways. Yan and Voth(Yan *et al.* 2004) also report that the electronic polarizability of ions can affect their dynamics. These are phenomena that will be absent in the present model, which considers only rigid ions of octahedral geometry and fixed charge distribution.

The exclusion of these phenomena is useful, however, in that it permits exclusive focus on the role of ionic charge distribution on dynamics. An enormous number of simulations of molten salts have been performed, both for simple binary salts(Trullás & Padró 1997; Trullás *et al.* 1991; Baranyai, Ruff, & McGreevy 1986; Sangster & Dixon 1976) and for molecular ILs of contemporary interest.(Margulis, Stern, & Berne 2002; Shah, Brennecke, & Maginn 2002; Yan *et al.* 2004; Hanke, Price, & Lynden-Bell 2001), However, other than

the studies of cyanide containing salts referenced above, we are not aware of any studies of salt systems that systematically explore the relationship between ionic charge distribution and dynamics. The present study considers ILs based on octahedral ions with structural parameters derived from the hexafluorophosphate ion. The PF_6^-. ion is incorporated in many ILs, but its use here is simply to provide a physically motivated model ion. The use of an octahedral ion (OI) in this context is desirable, as it represents the simplest geometric structure that permits independent distribution of charge along three coordinate axes, making it a good scaffolding on which distributions of charge can be incorporated. Once these basic principles connecting ionic charge distribution to liquid dynamics are understood, they can be used to aid the interpretation of experimental results and the design of ILs with superior properties.

2.2 Methodology

In this section, we describe the construction of the model systems used in the study and describe the methodology used in MD simulation.

2.2.1 The model molten salt

As described in the Introduction, our goal is to create rigid model ions that can be used to explore the relationship between the distribution of ionic charge and the dynamics of the liquid. All ions used in the present study possess octahedral symmetry in their mass distribution, as shown in Figure 2.1. The model is based loosely on the structure of PF_6^-, but is modified by the addition of atomic sites between the central atom and those at the end of each arm of the octahedron. These sites are referred to as "dummy" sites because they are assigned no short-ranged interaction potential and so do not affect dispersive interactions between neighboring ions. In some simulations, however, they are assigned charges

for reasons described below. We refer to the central site as a "P" site, the terminal site on each arm as a "F" site, and the intermediate site as a "Du" (Dummy) site. Lennard-Jones parameters for the P and F sites are identical to those for PF_6^- given in Margulis et al.(Margulis, Stern, & Berne 2002), and masses are assigned to each site to reproduce the total ionic mass and the moments of inertia of PF_6^- (see Table 2.1).

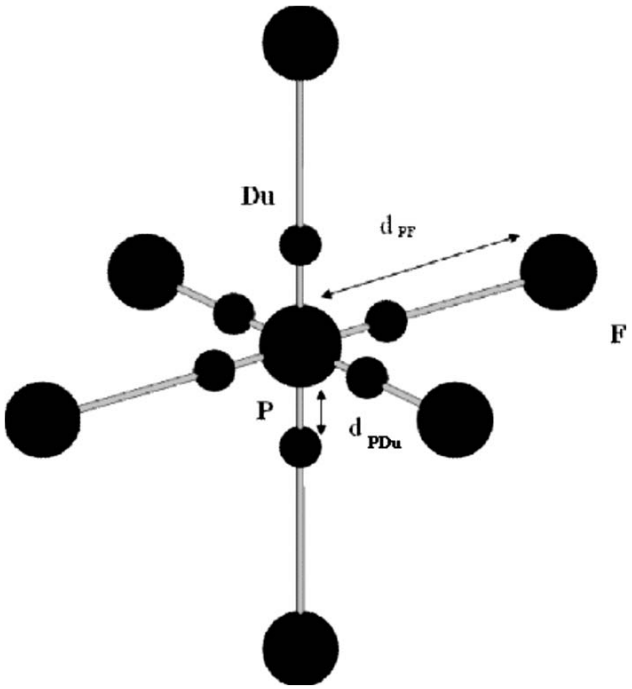

FIG. 2.1. Geometry of the model ions used in the present study.

This construction represents a scaffolding onto which different distributions of charge may be placed, permitting a study of how the distribution of charge affects dynamics. We construct four different ILs for simulation. We consider the simplest liquid first, and then explain how other liquids are constructed relative to it.

Anions were constructed by assigning charges to each of the sites. In the simplest case, which most closely resembles the PF_6^- ion, charges were assigned to the P and F sites and the Du sites were left neutral; see Table 2.2 for details. The P and F charges were

Table 2.1. Mass and geometric parameters for model ions.

Site Masses	
Site	Mass (amu)
F	18.67
P	15.00
Du	3.00
Bond Lengths	
Bond	Length (Å)
d_{PF}	1.637
d_{PU}	0.546

based on a computational study of (unmodified) PF_6^- carried out in the GAUSSIAN03 software suite.(Frisch *et al.* 2003) Calculations made use of density functional theory based on Beckes three-parameter gradient-corrected exchang(Becke 1993) and Lee-Yang-Parr gradient-corrected correlation functionals (B3LYP)(Lee, Yang, & Parr 1988) in the 6-31G(d,p) basis set. Atomic charges were calculated via the CHELPG algorithm.(Breneman & Wiberg 1990)

The ion with these charges assigned to P and F sites, with neutral Du sites, is designated OI_{Fs}. This indicates that it is an OI with charges at the F sites and a symmetric distribution of charge (i.e., the charges on all F sites are equivalent). Masses were assigned to each site to reproduce the total mass of PF_6^- and its moments of inertia.

Once the anion was constructed, a cation was created with a structure that was equivalent in all respects, but with charges of opposite sign. These two ions were combined to create a salt. The decision to create ILs in this way was motivated by a desire for simplicity, as ILs constructed this way have the fewest variables in their structure. The resultant cation is designated as OI_{Fs}^+ and the liquid resulting from the combination of the two is referred to as OI_{Fs}.

Because our prior work suggests asymmetry in charge distribution can affect dynamics,(Li *et al.* 2008) we created an IL analogous to OI_{Fs}, but with a small change in the

Table 2.2. Charge parameters for model anions. The symbols q_P, q_F and q_{Du} stand for the charges of the P, F and Du sites, respectively. In cases where charges are distributed asymmetrically, sites of a given type are denoted as single or double prime. Cations were constructed for each liquid by reversing the sign of the charge on each site of the anion.

	q_p(e)	q_F(e)	q_{Du}(e)
OI^-_{Fs}	0.931	-0.322	0.000
OI^-_{Fa}	0.931	$q_{F'}$=-0.422 $q_{F''}$=-0.222	0.000
OI^-_{Dus}	0.931	0.000	-0.322
OI^-_{Dua}	0.931	0.000	$q_{Du'}$=-0.622 $q_{Du''}$=-0.022

distribution of charge. The new liquid is designated OI_{Fa}, and is constructed by increasing the charges on three F sites (one on each axis) by 0.10, and decreasing the charge on the other three by the same amount to maintain the same total charge. Details are shown in Fig. 2.2 and Table 2.2. Both the cation and anion were changed in this way, so that the ions maintain distributions of charge that are equal in magnitude but opposite in sign. We will show in a later section that this relatively small change in the charge distribution has a significant effect on dynamics.

Two more species of ILs were constructed by placing charges at the Du sites and leaving the F sites uncharged. The anions are OI^-_{Dus} and OI^-_{Dua}, respectively, and each is combined with a cation. For OI^-_{Dua}, we increase the charge difference between different Du sites to 0.60 (see Table 2.2 for more detail). The motivation for this change was that the closer proximity of positive and negative charges tends to reduce their net interaction with neighboring ions in the same way that moving opposite charges together reduces the dipole of a neutral molecule. We chose the value of 0.60 so that the CLM would be the same for the OI_{Fa} and OI_{Dua} ions. This is an important question, as many ionic species (e.g., pyrrolidinium and tetraalkylammonium species) possess charge centers that are to some degree sterically hindered by aliphatic groups. The influence of such sterically hindered

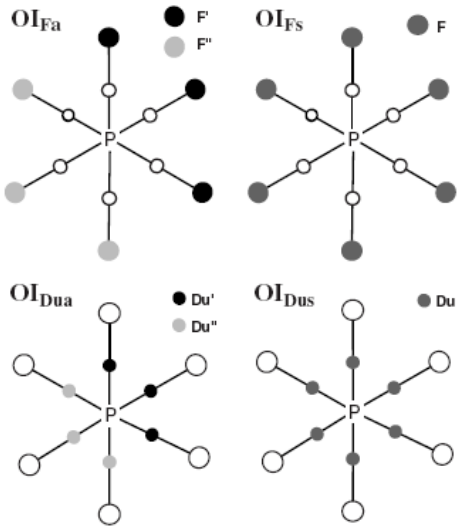

FIG. 2.2. Model anions used in the present study. The relative magnitudes of charges on F and Du sites are indicated by their shading; uncharged sites are denoted by empty circles

charge on dynamics is therefore an important question.

2.2.2 Simulation method

The system studied in this work consisted of 125 ion pairs (i.e. 250 ions in total). The simulations were performed with the DLPOLY(Smith & Forester 2001) software suite (version 2.13). Coulomb forces were calculated using an Ewald summation. Trajectories were integrated using the multi-timestep algorithm,(Forester & Smith 1994) with a timestep of 0.5 fs and long-ranged interactions recalculated at 2.5 fs intervals.

Trajectories were prepared from diffuse, random configurations by equilibration for 75 ps in an NPT ensemble using a Nóse-Hoover thermostat and an Anderson barostat at 500 K and 1 atm. Data was accumulated in a canonical (NVT) ensemble with the Nóse-

Hoover thermostat; each system was studied based on 12 independent trajectories each propagated for 1 ns.

2.3 Results and Discussion

2.3.1 Radial distribution functions

We first look at the OI_{Fa} and OI_{Fs} systems, in which the charge is symmetrically or asymmetrically distributed on the F-sites and the Du-sites are neutral. We show radial distribution functions (RDFs) for the ion centers of mass (the P-site) for cation-cation (P_{cat}-P_{cat}) and cation-anion (P_{cat}-P_{an}) in Fig. 3.3. The RDFs of P_{cat}-$P_{cat}$and P_{an}-P_{an} are equivalent by symmetry, so Pan-Pan is not shown. The RDFs for OI_{Fa} and OI_{Fs} exhibit strong spatial correlations consistent with expectations for a molten salt. The similarity of the RDFs for these systems suggests that the asymmetric charge distribution does not significantly affect the spatial distribution. The only detectable effect in the shape of the second peak of P_{cat}-P_{an} where the OI_{Fa} peak is sharper than its symmetric analog. A similar though less pronounced effect can be seen when comparing the RDFs for OI_{Dua} and OI_{Dus} in Fig. 3. This effect is interesting and its cause is unclear. However, the RDFs are very similar in all cases, suggesting that the details of the charge distribution do not greatly affect the structure.

2.3.2 Inhomogeneity

Many ILs are known to display structural inhomogeneity, and despite the similarities in the RDFs noted above it is worth exploring whether such features emerge in our model system. The spatial distribution can be characterized by the heterogeneity order parameter (HOP), as described by Voth et al.(Wang & Voth 2006) The HOP is defined as

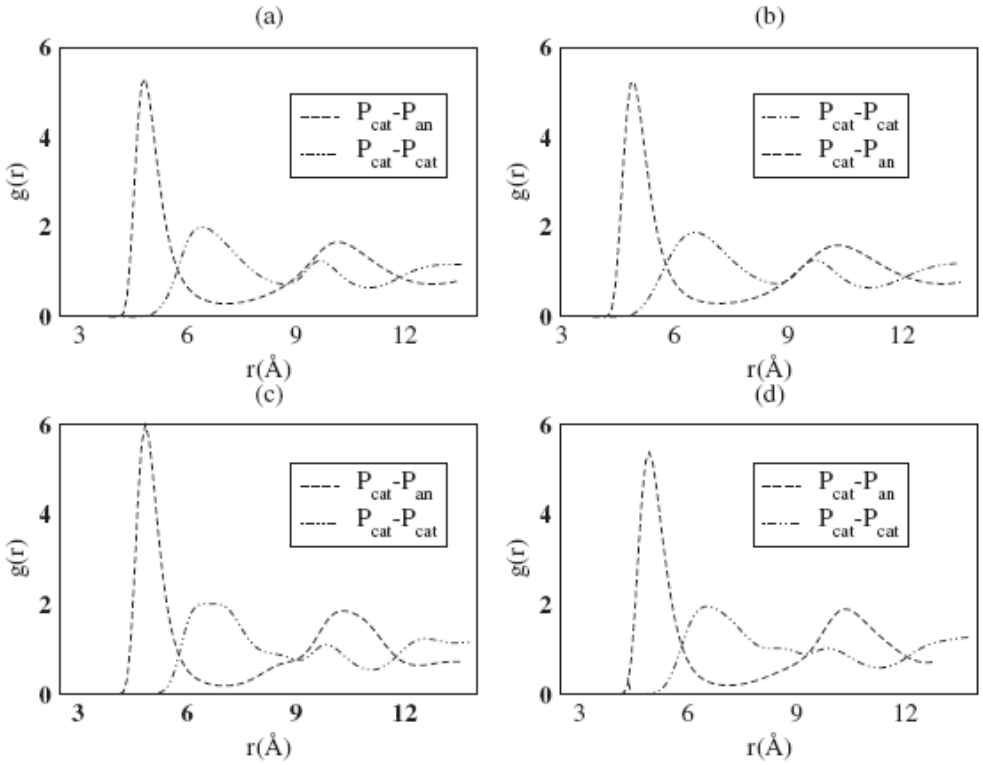

FIG. 2.3. Radial distribution functions for OIs with symmetric and asymmetric charge distributions.(a)OI$_{Dua}$,(b)OI$_{Fa}$, (c) OI$_{Dus}$, (d)OI$_{Fs}$.

$$h_i = \sum_j \exp(-r_{ij}^2/2\sigma^2), \tag{2.1}$$

where r_{ij} is the vector between the sites , $\sigma = L/N^{1/3}$,with L the side length of the cubic simulation box,and N is the total number of sites. Then the average HOP is calculated over the sites of interest N_s,

$$h = \frac{1}{N_s}\sum_{i=1}^{N_s} h_i, \tag{2.2}$$

For more discussion of HOP, the reader should review the cited reference. The re-

sults of the analysis for the present study are shown in Table 2.3. There is no significant difference between the HOPs associated with either of the symmetric ions and their asymmetric analogs, and only a very small difference between the models with charged F-sites and those with charged Du-sites. Thus, while it is possible that structural inhomogeneity may exist in the model, there is no evidence that it does and no indication that the charge distribution of the ions could influence it. This is consistent with the existing hypothesis about the origin of structural inhomogeneity in ILs, which attributes it to the presence of uncharged aliphatic substituents.

2.3.3 Orientational correlation functions

The rheology, electrical conductivity, and mass transfer properties of a liquid are important factors in determining the utility in a given application.(Arzhantsev *et al.* 2003; Angell 1984) A thorough study of the microscopic dynamics of ILs is therefore helpful in understanding how to design useful ILs.

Our previous work(Li *et al.* 2008) developed a quantity called the CLM to explore the correlation between ionic structure and IL dynamics. We made use of the center of charge description of the ion in which the electrostatic potential is approximated in a Taylor series expansion.(Wangsness 1986) The lowest order term in the expansion is assumed to be dominant, and represents the monopole (point charge) description of the ion. In this description, the relative positions of the center of mass and the center of charge determine the extent to which Coulomb interactions couple with rotational motion. According to this lowest-order description, Coulomb interactions do not couple rotational motion for the symmetric ions used in the present study. In the asymmetric cases, coupling is possible. The OI_{Dua} and OI_{Fa} models possess identical CLMs, and the CLMs of the symmetric species are zero by construction. Thus, any differences between the dynamics of the F-charged and Du-charged species must arise from the contributions of higher-order multipole moments.

Table 2.3. The Heterogeneity order parameter (HOP) for P_p-P_p distribution in 4 IOs models.

	HOP
OI_{Fs}	8.740
OI_{Fa}	8.677
OI_{Dus}	9.085
OI_{Dua}	9.050

Comparison of the models presented here therefore offers some insight on the validity of the center of charge description of ILs.

Insight into the microscopic rotational motion of the ions can be gained by study of the orientational correlation functions (OCFs),

$$\Omega_m(t) = \langle i_m(t) \cdot i_m(0) \rangle, \tag{2.3}$$

where the $i_m(t)$ are the time-dependent unit vectors (m=X,Y,Z).Since each axis of the molecular frame in the OIs is equivalent based on our construction, we report a single quantity in the OCFs calculation.

The OCFs are calculated for each model and are shown as Figure 3.4. The data are averaged over 1 ns. The relaxation times τ_m, shown in Table 2.4,have been calculated by fitting $\Omega_m(t)$ to an exponential function.

The parameter C is included to account for long-lived decay components that are inaccessible on the time scale of the simulation. Such long-lived components are well-known in both experimental (Arzhantsev *et al.* 2006) and theoretical(Ribeiro, de Oliveira, & Gonçalves 2001) studies of ILs. They are present as a small but significant contribution to the dynamics for the asymmetric cases reported here, though we do not characterize them in detail due to the challenge posed by such long time scales.

The OCFs of $OI_{Fa}$and OI_{Dua} decay more slowly than their symmetric analogs, an

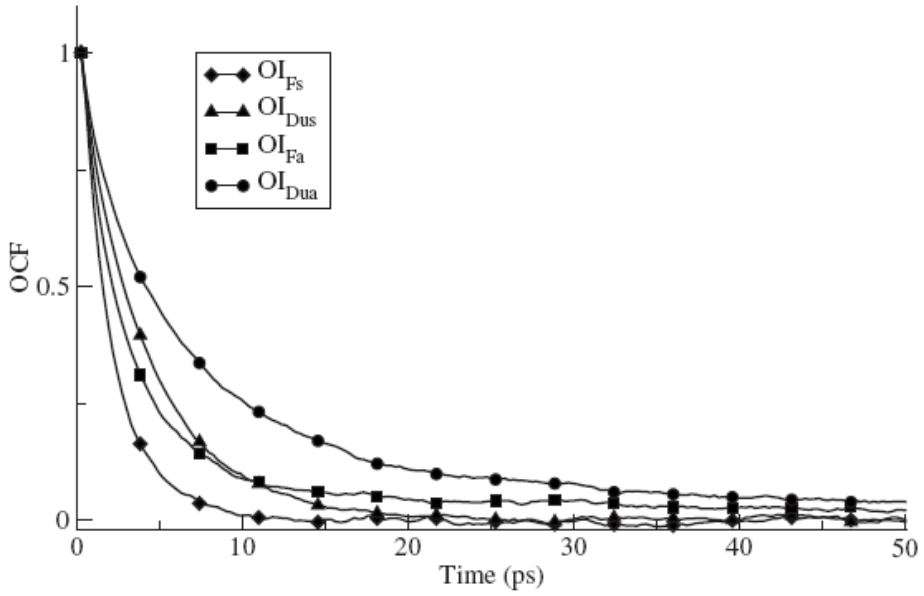

FIG. 2.4. OCFs for the model systems. Symbols are used only to identify data sets, and are not reflective of the density of points.

effect we attribute to the mixing of rotational and translational motion. That is, asymmetry in the distribution of charge can make it necessary for an ion to translate relative to its neighbors in order to bypass a barrier to rotation. Ionic translational diffusion is often slow in molten salts, and so will act to slow rotational motion. The much weaker Coulomb-coupling to libration in the $\mathrm{OI}_{Fs}$and OI_{Dus} cases implies that ions rotate relatively freely.

Coupling of$\mathrm{OI}_{Fa}$and OI_{Dua} rotational dynamics with collective vibrational modes is consistent with the existence of long-lived components of the OCFs for asymmetric ions evident in Fig.3.4. Interion vibrational modes are known to exist in ILs with lifetimes of hundreds of picoseconds or even nanoseconds. While the OCFs for the symmetric species have decayed to zero by 50 ps, correlations persist for the asymmetric species due to cou-

Table 2.4. The relaxation time of the orientation correlation functions of 4 OIs models. The naming scheme for the 4 ionic liquids and related discussion can be found in the text.

	τ_m (ps)
OI_{Fs}	1.96
OI_{Fa}	3.26
OI_{Dus}	4.06
OI_{Dua}	7.16

pling with these long-lived modes.

Urahata and Ribeiro(Urahata & Ribeiro 2005) have reported the anisotropy and reorientational relaxation of the ILs incorporating the imidazolium cation. Their results indicate that the presence of a long alkyl chain on the imidazolium restricts rotation about axes orthogonal to it, but does not greatly hinder rotations about the axis defined by the direction of the chain. This is broadly consistent with our results, in that a more symmetric distribution of charge about a given axis permits freer rotation. However, the greater structural complexity and flexibility of the imidazolium ions in the Urahata and Ribeiro study complicate comparison to the present simulations.

It is tempting to draw an analogy with dielectric friction in molecular liquids, though some caution is in order in this comparison. In molecular liquids, dielectric friction occurs when a dipolar molecule is immersed in a polar liquid, and the electrostatic polarization of the medium acts to retard rotation. Analogous interactions surely exist for an ion immersed in an IL, though the nature of the interactions are ion-ion rather than dipole-dipole as occur in molecular liquids. However, were the role of the surrounding liquid simply to polarize and retard the motion of solute charges, there would be no reason to expect the translational diffusion of asymmetric species to be more rapid than that of symmetric species, as both types of ions should be similarly “pinned” through interactions with the surrounding medium. Yet as we show before, liquids composed of asymmetric ions do indeed show more rapid self-diffusion than their symmetric analogs. This is explained (as

noted above) by interpreting the solvent response as incorporating the ion into collective motion that mixes translational and librational motion, a more subtle phenomenon than dielectric friction per se.

It is interesting to note that the OCFs decay faster for the species $OI_{Fs}$and OI_{Fa} than for cases in which charge is distributed on Du sites. This is counterintuitive, as it means a greater localization of charge at the surface of the ion acts to increase the rate of rotation. This is a phenomenon that must be associated with higher-order multipole moments of the ionic charge distribution. The physical reason for the behavior may involve coupling to higher frequency collective modes of the liquid, which may interact more strongly with the more diffuse charge distribution. We return to this point in next subsection.

2.3.4 Self-diffusion behavior for model ions

The diffusion of ions in a liquid is conventionally described through the mean square displacement (MSD)

$$\langle \Delta |r(t)|^2 \rangle = \frac{1}{N} \langle \sum_{i=1}^{N} |r_i^c(t) - r_i^c(0)|^2 \rangle, \tag{2.4}$$

which is calculated from the center-of-geometry (P-site) r_i^c of the OI ions. Figure 2.5 shows the MSD at 500K for our four model liquids.It is reported in simulations of other ILs(Hanke, Price, & Lynden-Bell 2001; Margulis, Stern, & Berne 2002) that the initial dynamics are ballistic, followed by diffusive behavior on longer time scales. We see similar behavior with significantly different rates of diffusion on different timescales. We see rapid initial diffusion in the first 100 ps, followed by slower diffusion on intermediate timescales(roughly 100 ps to 350 ps) and finally linear diffusion. This diffusion pattern is consistent with the result of other simulation of ionic liquids.(Yan *et al.* 2004; Del Pópolo & Voth 2003; Wang & Voth 2006)

The asymptotic diffusion constants of each IL are calculated from the slopes of MSD between 800 and 1000 ps, and are reported, along with their standard deviations, in Table 2.5. Clearly, the diffusion constants are higher for model ions possessing an asymmetric charge distribution than for their symmetric analogs. This implies that asymmetry plays an important role in the diffusive behavior of ions in a fused salt. This result is consistent with our previous work(Li *et al.* 2008) in that the asymmetric charge distribution implies a higher CLM, which was found in that work to be associated with more rapid experimental transport properties.

Curiously, the ILs with charges on the dummy atoms (OI_{Dus} and OI_{Dua}) diffuse more slowly than those with charges on the F-sites. This is a counterintuitive result given that one would expect the F-charged ions to display stronger interion Coulomb interactions, and therefore diffuse more slowly. The CLM approach would not account for this effect, and would predict the $OI_{Fa}$and OI_{Dua}ions to diffuse at the same rate on the grounds that they possess the same CLM. The origin of the more rapid diffusion of the F-charged species may arise from the coupling to collective motion noted previously for the OCFs, a point discussed below.

2.4 Conclusion

In this paper the structural and dynamic properties of a model molten salt system have been studied by MD simulation. We find that while changes in the charge distribution of symmetric ions do not alter liquid structures, they have a profound effect on dynamics. The RDFs indicate that liquid structures are not highly sensitive to ionic charge distribution. We also find no evidence of structural inhomogeneity in the model system, and examination of the HOP reveals that if any inhomogeneous structures are present they are not affected by the distribution of ionic charge in this model.

Table 2.5. The slope of the MSD and the calculated diffusion constants for the model ILs. Values are based on analysis of the data at times between 800 and 1000 ps to ensure convergence of the dynamics. Standard deviations are included

	slope($\times 10^{-3} \cdot \mathring{A}^2$/ps)	diffusion coefficient($\times 10^{-4} \cdot \mathring{A}^2$/ps)
Charge on Fluorine atoms		
OI_{Fs}	1.87 $\pm$ 0.22	3.12$\pm$0.37
OI_{Fa}	23.18$\pm$ 0.18	38.63$\pm$ 0.30
Charge on dummmy atoms		
OI_{Dus}	0.24$\pm$ 0.12	0.39$\pm$0.20
OI_{Dua}	12.31$\pm$0.15	20.52$\pm$0.25

However, the dynamic properties of the fused salts are very sensitive to the charge distribution within the ions. The OCFs indicate that librational correlations decay more slowly for asymmetric species than for their symmetric analogs, and studies of translational diffusion indicate that asymmetric ions diffuse more rapidly. Both of these phenomena can be attributed to the stronger Coulomb interactions coupling rotational and translational motion for the asymmetric species. In the absence of such coupling, rotation is a relatively rapid motion and diffusion is slow. The presence of this coupling mixes the modes, slowing rotation and increasing the rate of diffusion.

This interpretation is consistent with our earlier work on the CLM, where we observed that significant asymmetry in the charge distribution of ions was associated with a reduced viscosity. The simulations thus validate the key qualitative features of the model. However, the CLM approach does seem to fail when comparing the F-charged species to the Du-charged species. A strict CLM interpretation would predict that the dynamics of both asymmetric species should be the same, as the CLMs are the same. This should also be true for the symmetric species, where the CLM is zero.

Given its simplicity, some degree of failure in the model is to be expected. However, one might anticipate that this failure would arise from stronger interion interactions associated with the F$-$charged species, which would be expected to retard ionic dynamics. In

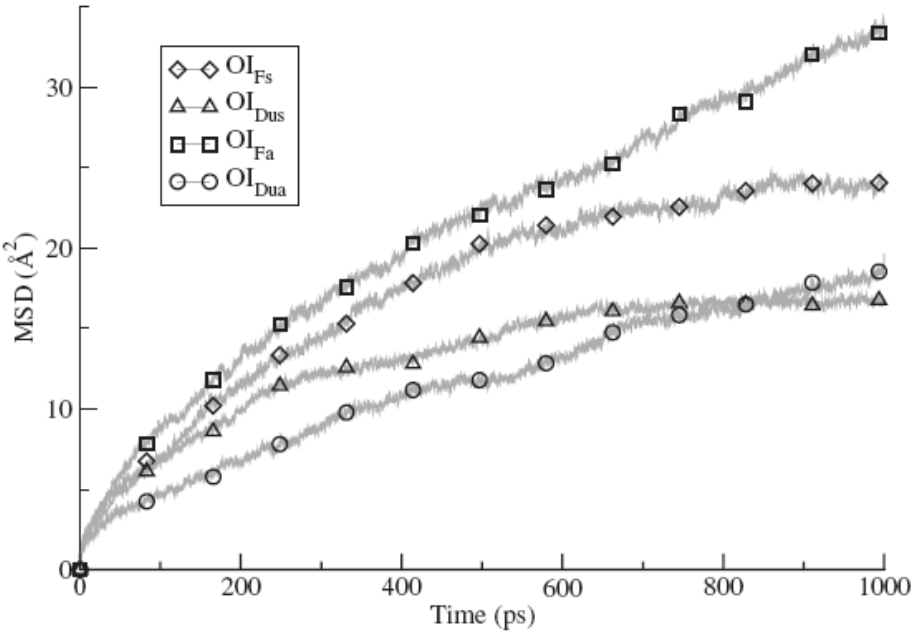

FIG. 2.5. MSDs for ions in the four ILs. Symbols are used only to identify data sets and are not reflective of the density of points.

fact, the F−charged species show more rapid libration and translational diffusion.

The most likely explanation for this phenomenon lies in the collective motion of the liquid. This has been characterized in other contexts,(Kobrak 2006; 2007) and is found to dominate molten salt dynamics on all but the shortest time scales. The more diffuse charge distribution associated with the F-charged species dictates that those species possess larger electrostatic quadrupole and higher order multipole moments than the Du-charged species. These higher-order terms may possess the correct symmetry to couple with highly symmetric collective modes of the liquid, altering liquid dynamics.

Such coupling is not typical of molecular liquids, where collective dynamics are in most cases dominated by dipole-dipole interactions. However, one must consider that ion-

quadrupole interactions display the same distance$-$dependence (r^{-3}) as dipole-dipole interactions.It is already known that ion-quadrupole interactions (in the form of cation$-\pi$ interactions) strongly influence solvation properties in ILs.(Hanke & Lynden-Bell 2003) It is thus plausible that quadrupole terms, and perhaps even higher-order terms, could influence collective dynamics in fused salts. The more rapid dynamics of the F-charged species may therefore reflect coupling to certain relatively high-frequency modes of high symmetry.

The importance and ubiquity of such quadrupolar coupling in real ILs is unclear. For all that these model ions are based on the structure of PF_6^-., they do by design represent extremes in the distribution of charge and do not possess certain characteristics of real molecules. Phenomena such as ionic polarizability and flexibility may "blur" the charge distribution and reduce the effective magnitude of an ionic quadrupole, reducing the strength of coupling to collective motions. Nevertheless, the possibility that such ion-quadrupole interactions could be a significant determinant of collective dynamics is intriguing, and will be the subject of future work.

Chapter 3

INSTANTANEOUS NORMAL MODE ANALYSIS OF A PAIR OF MODEL MOLTEN SALTS

abstract We have investigated how the distributions of mass and charge in an ion of a fused salt affect liquid dynamics using analytical theory and a series of molecular dynamics (MD) simulations. The translational and rotational motion of ions and their coupling have also been studied. In this chapter, we investigate ionic liquid dynamics using instantaneous normal mode (INM) analysis. The translational and rotational contributions to each INM mode are calculated. The coupling of both motions are discussed and compared with the MD simulations in Chapter 2.

3.1 Introduction

In recent years, instantaneous normal mode (INM) analysis has been used as an important tool in analyzing dynamical properties of molecular liquids.(Stratt & Cho 1994; R.Stratt 1995; S.Ryu & R.Stratt 2004; T.Keyes 1997) The ability of INM theory to provide a comprehensive analysis of dynamics at short (subpicosecond) time intervals has been acknowledged and the method has been used to study ultrafast solvation dynamics,(Ladanyi & Stratt 1995),glass transitions(S.D.Bembenek & B.B.Laird 1996),optical Kerr effect spectra(T.Keyes 1997; S.Ryu & R.Stratt 2004),and cluster dynamics.(J.E.Adams & R.Stratt

1990)

In this chapter, we apply the instantaneous normal mode analysis to the system of model molten salts described in the previous chapter. We compute the INM spectra for symmetric and asymmetric ILs and calculate the separate translational and rotational contributions to each instantaneous normal mode using appropriate projection operators. We then analyze the results of the INM approach to describe specific ionic motions in the liquids and interpret the coupling between the translational and rotational motion in symmetric and asymmetric molten salt species.

To the best of our knowledge, the INM approach has not been applied in any ILs. Ribeiro et.al(Ribeiro & Madden 1997) carried out an INM calculation on alkali halide-based ionic melts in six distinct thermodynamic states and reported the ratio between the cation and anion self-diffusion coefficients. The self-diffusion behavior is then interpreted by considering the INM density of states. The unstable mode, which they claimed to be related to barrier crossing on the topological potential energy surface, is a small fraction of the total imaginary frequency modes, while the real branch of INM density of states (DOS) represents the quenched configuration DOS. Stratt et.al(M.Buchner, B.M.Ladanyi, & R.Stratt 1992)have used the INM approach to the system of model diatomic molecules in liquids. The autocorrelation function calculated from INM theory showed a good agreement with molecular dynamics simulation results in the condition that the analysis is constrained in short enough time. The nature of the translational-rotational coupling is reported by calculating the the specific translational and rotational projections of the modes. The negative proportion of both translational- and rotational-velocity autocorrelation functions is reported and interpreted in instantaneous harmonic modes.

It must be noted that there are still controversy on using the INM approach to predict the barriers to the self-diffusion behavior by looking at the unstable modes of the liquids.(J.D.Gezelter, E.Rabani, & B.J.Berne 1997; T.Keyes 1994) We will return to this

issue in our discussion of data analysis in this chapter.

In section 3.2, we introduce the INM theory briefly and discuss simulation methodology. In section 3.3, we present the data and the analysis, including the density of states of normal modes and the projected translational and rotational motions. The liquids dynamics are also discussed. It is shown that rotational behavior of both model salts described by INM approach is consistent with the MD simulation results introduced in chapter 2, while the translational motion is more complicated and will be discussed in detail in section 3.3.2.

3.2 Methodology

3.2.1 Instantaneous Normal Modes for nonlinear ion pairs

The theory of instantaneous normal modes relies on the idea that at sufficiently short times liquids which are in an equilibrium state can be viewed as moving in a harmonic force field and can be interpreted in the framework of normal modes.(T.Keyes 1994; 1997)If we consider a set of rigid ions with molecular weight M, the Hamiltonian of a liquid composed of these ions can be expressed as

$$H = \sum_{i=1}^{N}(\frac{1}{2}M\dot{r}_j^2 + \frac{1}{2}\sum_{i=x,y,z} I_{ji}\omega_{ji}^2) + V(R) \tag{3.1}$$

where r_j is the center$-$of$-$mass of the jth ion (j=1,...,N) and $\omega_{ji}$and I_{ji} are the angular velocity and the moment of inertia about the i axis of the jth ion respectively. The last term of the Hamiltonian is the potential energy, which depends on the liquid configuration $\mathbf{R}$.

$$\mathbf{R} = [\mathbf{r_1}, \mathbf{\Omega_1}, ..., \mathbf{r_N}, \mathbf{\Omega_N}], \tag{3.2}$$

with $\mathbf{r_j}$=X_j,Y_j,Z_j which are Cartesian coordinates and $\mathbf{\Omega_j}$=ϕ_j,θ_j,ψ_j the Euler angles. The $6N$-dimensional mass-weighted coordinates can be defined as

$$Z = [z_{11}, z_{12}, ..., z_{ji}, ..., z_{6N}] \tag{3.3}$$

with

$$z_{ji} = [\sqrt{M}x_j, \sqrt{M}y_j, \sqrt{M}z_j, \sqrt{I_x}\zeta_{jx}, \sqrt{I_y}\zeta_{jy}, \sqrt{I_z}\zeta_{jz},], \tag{3.4}$$

for i=1,2,...,6, and the mass-weighted angular velocities can rewritten in Euler angle matrix. In the mass-weighted coordinates, the new Hamiltonian can rewritten in the form

$$H = \frac{1}{2}\dot{Z}\cdot\dot{Z} + V(\mathbf{R_0}) - F(\mathbf{R_0})\cdot(Z_t - Z_0) + \frac{1}{2}(Z_t - Z_0)\cdot D(\mathbf{R_0})\cdot(Z_t - Z_0), \tag{3.5}$$

where the $F(\mathbf{R_0})$ and $D(\mathbf{R_0})$ are the $6N$-dimensional force vector and $6N\times6N$ mass-weighted dynamical matrix in the form

$$F_{ji}(\mathbf{R_0}) = -(\nabla_{ji}V)_{\mathbf{R_0}} \tag{3.6}$$
$$D_{ji,j'i'}(\mathbf{R_0}) = -(\nabla_{ji}\nabla_{j'i'}V)_{\mathbf{R_0}}$$

Where $\nabla_{ji} = \dfrac{\partial}{\partial z_{ji}}$.

Consider the $6N\times6N$ orthogonal transformation matrix $\mathbf{U}(\mathbf{R_0})$ which can diagonalize the dynamical matrix(i.e. the Hessian). The eigenvalues of the Hessian can be calculated as

$$\omega_\alpha^2(\mathbf{R_0}) = \sum_{ji,j'i'} U_{\alpha,ji}(\mathbf{R_0})D_{ji,j'i'}(\mathbf{R_0})U_{\alpha,j'i'}(\mathbf{R_0}), \tag{3.7}$$

It should be noted that the value ω_α^2 can be negative, implying an imaginary frequency. The modes with these frequencies are called imaginary modes and are depicted on the negative frequency axis in plots of the density of states. The imaginary modes are usually accepted

as unstable modes in INM analysis, corresponding to transport rather than bound harmonic motion. We will review this topic in more detail at the end of this section.

The instantaneous normal coordinates can be defined as

$$q_\alpha(t, \mathbf{R_0}) = \sum_{ji} U_{\alpha,ji}[z_{ji}(t) - z_{ji}(0)] \tag{3.8}$$

Using the instantaneous normal coordinates, the Hamiltonian corresponding to given configuration $\mathbf{R_0}$ becomes

$$H = V(\mathbf{R_0}) + \sum_{\alpha=1}^{6N}(\frac{1}{2}\dot{q}_\alpha^2 + \frac{1}{2}\omega_\alpha^2 q_\alpha^2 - f_\alpha q_\alpha). \tag{3.9}$$

In other words, the system is harmonic. In this approximation, the probability distribution of the instantaneous normal modes can be described by liquid's density of states

$$D(\omega) = \langle \frac{1}{6N}\sum_{\alpha=1}^{6N}\delta(\omega - \omega_\alpha)\rangle \tag{3.10}$$

where the bracket means the equilibrium average over the liquid configurations.

In order to characterize the translational and rotational degrees of freedom in the total density of states, the projectors of the corresponding motions can be defined

$$\begin{aligned} P_\alpha^T &= \sum_{j=1}^{N}\sum_{i=1,2,3}(U_{\alpha,ji})^2 \\ P_\alpha^R &= \sum_{j=1}^{N}\sum_{i=4,5,6}(U_{\alpha,ji})^2. \end{aligned} \tag{3.11}$$

Then the translational and rotational densities of states can be separated as

$$D^T(\omega) = \langle \frac{1}{6N}\sum_{\alpha=1}^{6N} P_\alpha^T\delta(\omega - \omega_\alpha)\rangle \tag{3.12}$$

$$D^R(\omega) = \langle \frac{1}{6N} \sum_{\alpha=1}^{6N} P_\alpha^R \delta(\omega - \omega_\alpha) \rangle.$$

Clearly, because of the orthogonality of the transformation matrices, the translational and rotational densities of states obey the rule

$$D^T(\omega) + D^R(\omega) = D(\omega) \tag{3.13}$$

It is easy to show that the projectors yield the relative contribution of translational and rotational motion to the total density of states at each value of ω. The goal of this study is to understand how these motions influence liquid dynamics.

It must be noted that even though the INM theory has been known for several decades and has been proved to be a powerful tool for analyzing liquid dynamics, there is still some controversy on one specific aspect of the theory. Specifically, it has been widely accepted that the real frequency of INM mode is due to the short lifetime harmonic oscillations around a local minimum of a potential well, while the imaginary frequency is corresponds to dynamic at a saddle point between them shown as Figure 3.1. Keyes(T.Keyes 1994) analyzed the unstable mode of a broad range of supercooled and normal liquids and developed a function related to the topological potential surface. He used this function to characterize energy barriers to liquid diffusion and elaborate on Zwanzig's basin-hopping model(Zwanzig 1983), based on a model for hopping times between basins and knowledge of the unstable modes in INM. However, Berne et al.(J.D.Gezelter, E.Rabani, & B.J.Berne 1997) disputed the ability of imaginary instantaneous normal modes to predict the barrier height to the self-diffusion. The authors argued that Keyes' work can only be correct based on several assumptions, but these assumptions are not necessarily true in all liquid systems.

Even though we do not go into the question of how the controversy can be resolved, the discussion cited above is related to the discussion of INM data given below.

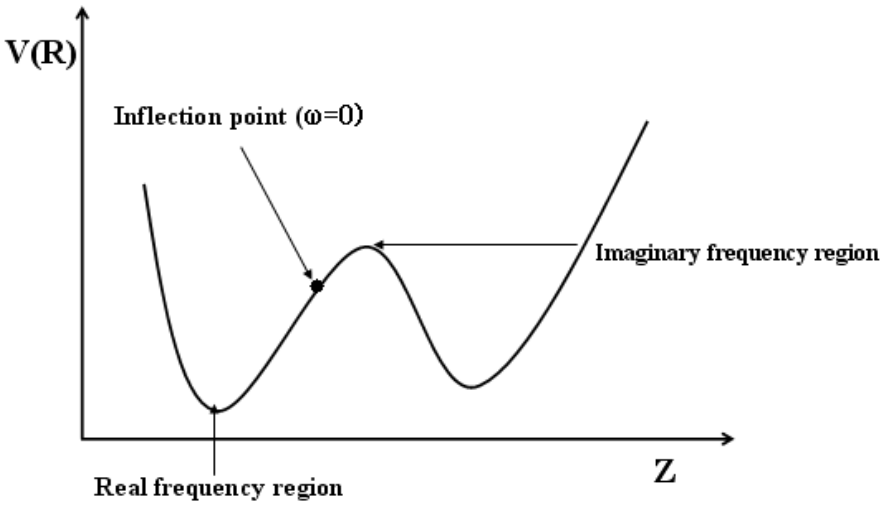

FIG. 3.1. The potential landscape describing the correspondence of real and imaginary frequencies in INM theory.

3.2.2 The model molten salt and simulation techniques

The model molten salts we consider in this INM study are the same OI_{Fa} and OI_{Fs} given in the previous chapter. The simulations are similar to previous work, but a smaller simulation cell is used to facilitate matrix calculations. The system size includes 64 ion pairs (128 ions) for each molten salt. All other parameters with regard to force field and timestep are the same. The Hessian matrix is calculated every 5 fs during simulation, based on trajectory data taken over 5 ps (i.e. 1000 configurations for each salt).

3.3 Data and Discussion

3.3.1 Density of states

We first calculate the density of states (DOS) of the two model molten salts and apply the rotational and translational projection operators to the normal modes. The results with the specific translational and rotational projectors are shown in Fig.3.2. The projected translational motion is the solid line while the rotational motion is described by the dashed line. The real frequency portion of the spectra is very similar for both the symmetric and asymmetric molten salts, showing nearly identical lineshapes. Subtle differences exist in the negative frequency range, shown in more detail in Figure 3.3.

Looking at the rotational and translational component, it is clear that the rotational component dominates in the negative part of frequency spectrum and at low frequencies in the real region, while the translational component rises above the rotational motion at high real frequencies. The phenomenon suggests that rotational motion is less hindered than translational motion in both molten salts.

Looking in more detail in negative portion of the spectrum in Fig 3.3, it is clear that the asymmetric model shows a broader spectrum in the rotational component, while its translational component displays a slight shift towards ω=0. The first indicates that the rotation of symmetric model is less hindered. This is consistent with the molecular dynamics simulations reported in the last chapter, in which the same model displays a significantly faster decay of rotational correlations than its asymmetric analog. The latter finding is interesting and deserves deeper consideration. We attribute this different population in translational imaginary frequency to different barrier height of self-diffusion and the lower potential energy of the inflection point in asymmetric model. We will discuss this issue in the following section.

3.3.2 Translational and rotational projectors

As explained in section 3.2, the translational and rotational projectors can be calculated and are displayed in figure 3.4. The upper figure shows the rotational projection for each model and the lower figure shows translational projection. The projectors all show a strong dependance on frequency in the real portion in the frequency range, though the behaviors are nearly identical for the symmetric and asymmetric models. In the negative range, the projected motion is more complicated. The rotational component of the asymmetric model is larger than the rotational component of the symmetric model at most negative frequencies, but the situation changes near ω=0. However, for the translational projectors the trend is reversed.

The observation that both translational and rotational projections change their trend between asymmetric and symmetric models near ω=0 is interesting and deserves a more careful discussion. Xu et.al(Xu, Cooper, & Angell 2003) have reported that ionic liquids are glass formers and form amorphous solids when cooled. The glass-forming ILs can be viewed as occupying a series of local minima on a potential landscape. The dynamics of the liquids can be elucidated by the activated transition between these minima.(Sastry, Debenedetti, & Stillinger 1998) What is more, when comparing the translational and rotational contributions for two IL models in Figure 3.2 we notice that the point where they differ most significantly is located at the peak of DOS for the imaginary frequency. In other words, in the spectral region where the highest population of unstable modes exist. As we have discussed in section 3.3.1, the unstable mode is important in describing the transport properties in liquids. Therefore, we attribute the low magnitude frequency modes in the negative frequency range as the modes that determine transport behavior in ILs. The translational character of the modes in this region is higher for the asymmetric model than for the symmetric model, indicating that a greater fraction of the motion is translational. This

must explain higher rate of diffusion in the model salts. In this point of view, the structure of the region near ω=0 in the imaginary frequency range implies that translational motion is less hindered in the asymmetric model than in the symmetric one, which is consistent with the MD results for the translational diffusion in chapter 2.

3.3.3 Population of modes and inflection point

We note that at the point where the frequency equals zero a peak is observed in both models, shown in the Figure 3.5. Similar peaks are found in other INM studies.(J.D.Gezelter, E.Rabani, & B.J.Berne 1997; R.Stratt 1995; Ribeiro & Madden 1997) We attribute the peak to population at the inflection point of the potential energy, which separates the stable and unstable mode regions of the potential topography shown in Figure 3.1. The height of the peak indicates the population of the modes located in the inflection point. The fact that the peak in ω=0 for symmetric and asymmetric models does not show a significant difference suggests that the total population of modes in the inflection point are similar for both models. However, the projection operators at ω=0 are quite different in the two models, with a higher relative population in the translational component of the asymmetric mode. This may be associated with diffusive transport, as ions may more through an inflection point during an activated process.

To our knowledge, the role of modes with ω=0 has not been discussed in detail in the literature. A peak at ω=0 is observed in some systems but not in others, as noted in Table 3.1. As mentioned in the previous paragraph, we speculate that the ω=0 mode is associated with transport in ILs, but do not attempt a detailed interpretation of the structure here.

Table 3.1. Appearance of peak at ω=0 in INM analysis in various other studies.

System	Appearance of ω=0 peak	Reference
Ar(g)	yes	(J.D.Gezelter, E.Rabani, & B.J.Berne 1997)
H_2O	no	(M.Cho, G.R.Fleming, & R.M.Stratt 1994)
Alkali halide	yes	(Ribeiro & Madden 1997)
Benzene	no	(S.Ryu & R.Stratt 2004)
CS_2	no	(Li & T.keyes 1997)
OI salts	yes	This work
Diatomic molecule	yes	(M.Buchner, B.M.Ladanyl, & R.M.Stratt 1992)

3.4 Conclusion

We have analyzed the symmetric and asymmetric model salts introduced in the previous chapter using the instantaneous normal mode approach. The density of states of the normal modes is calculated to analyze the dynamics of the salts.

In order to interpret the translational and rotational motions between the two model salts, the translational and rotational contributions to each instantaneous normal mode have been calculated using appropriate projection operators. It has been found that that the rotation of the symmetric model is faster than its asymmetric analog, which is consistent with the molecular dynamics simulations reported in previous chapter.

The imaginary low frequency spectrum near ω=0 appears to be significant in describing the transport properties in both salts due to the glassy dynamics of ILs. In this range of imaginary frequencies, the asymmetric model possesses a higher proportion of translational motion than its symmetric analog, consistent with the data for ionic self-diffusion reported in chapter 2.

There is also evidence that modes near ω=0 associated with motion at the inflection point may contribute significantly to diffusion. This is based on the observation that the INM spectra of the two salts are nearly identical except in this region, and they display significantly different transport behavior. This observation may be of interest in interpreting

the result of other studies.

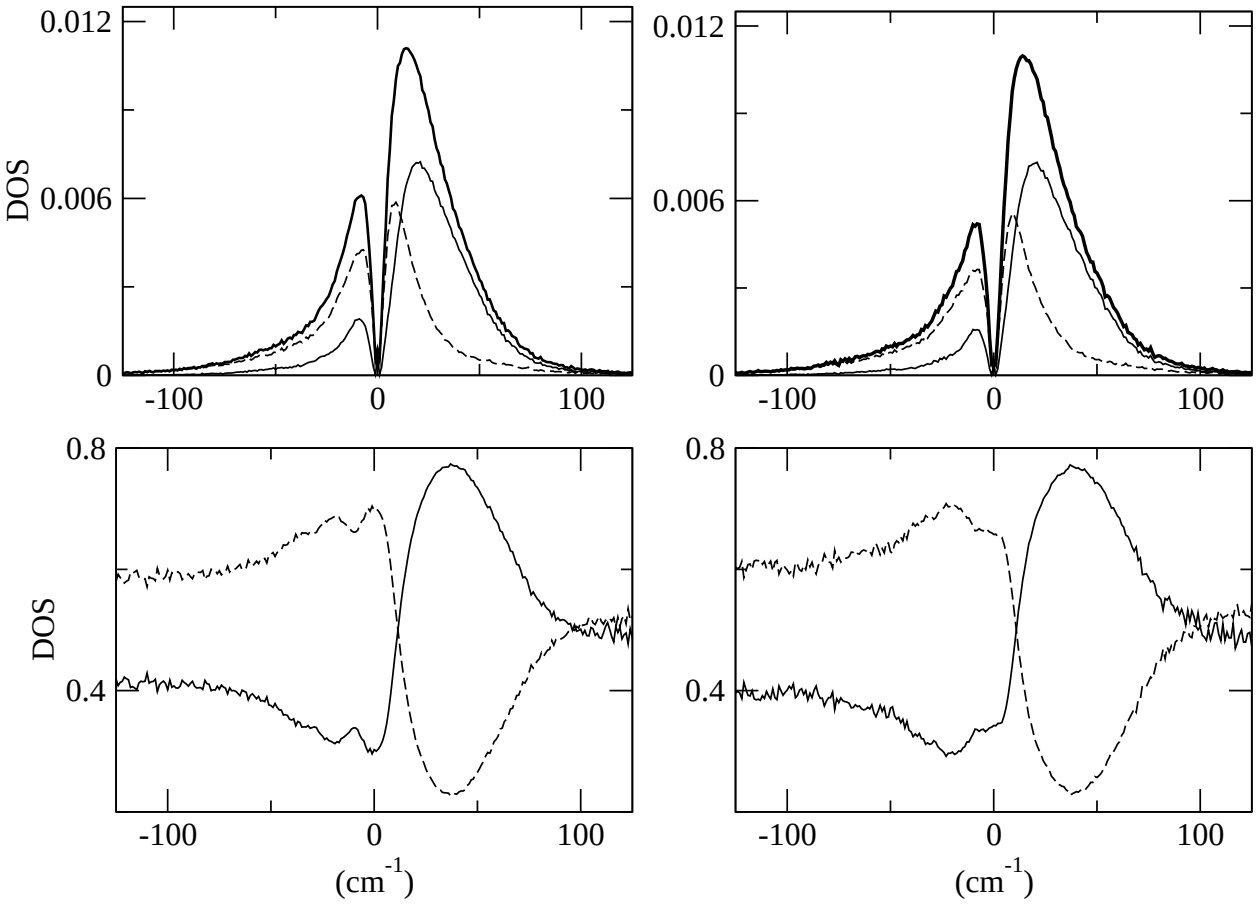

FIG. 3.2. The density of states of two model molten salts, with corresponding projectors of translational and rotational motion in the second row. The symmetric model salt is displayed in the left column and the asymmetric one is in the right column. The projected translational motion is the solid line while the rotational motion is described by the dashed line. The bold solid line is for the total density.

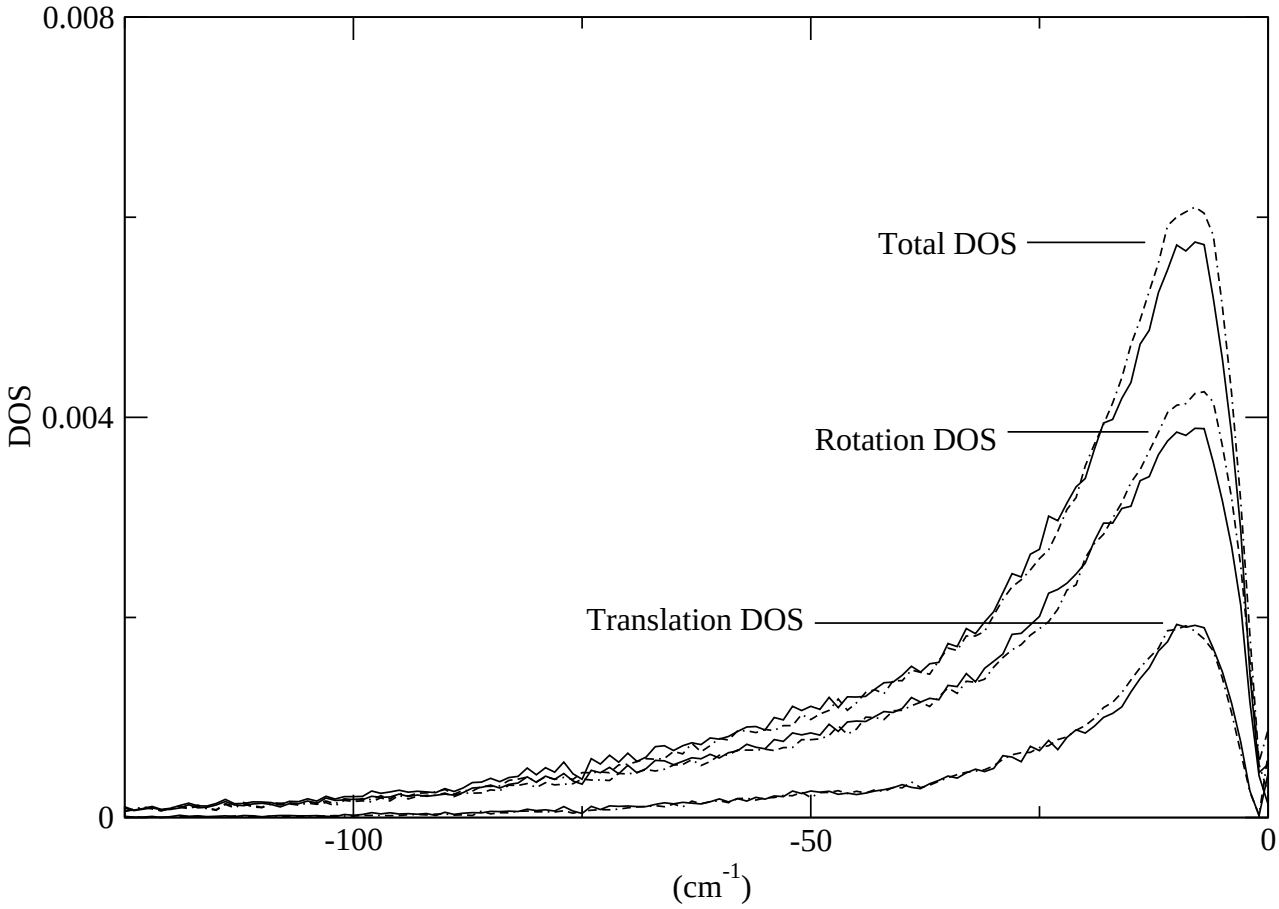

FIG. 3.3. Negative frequency portion of density of states for two molten salts, with the a solid line indicating the asymmetric model and the dashed line for the symmetric model.

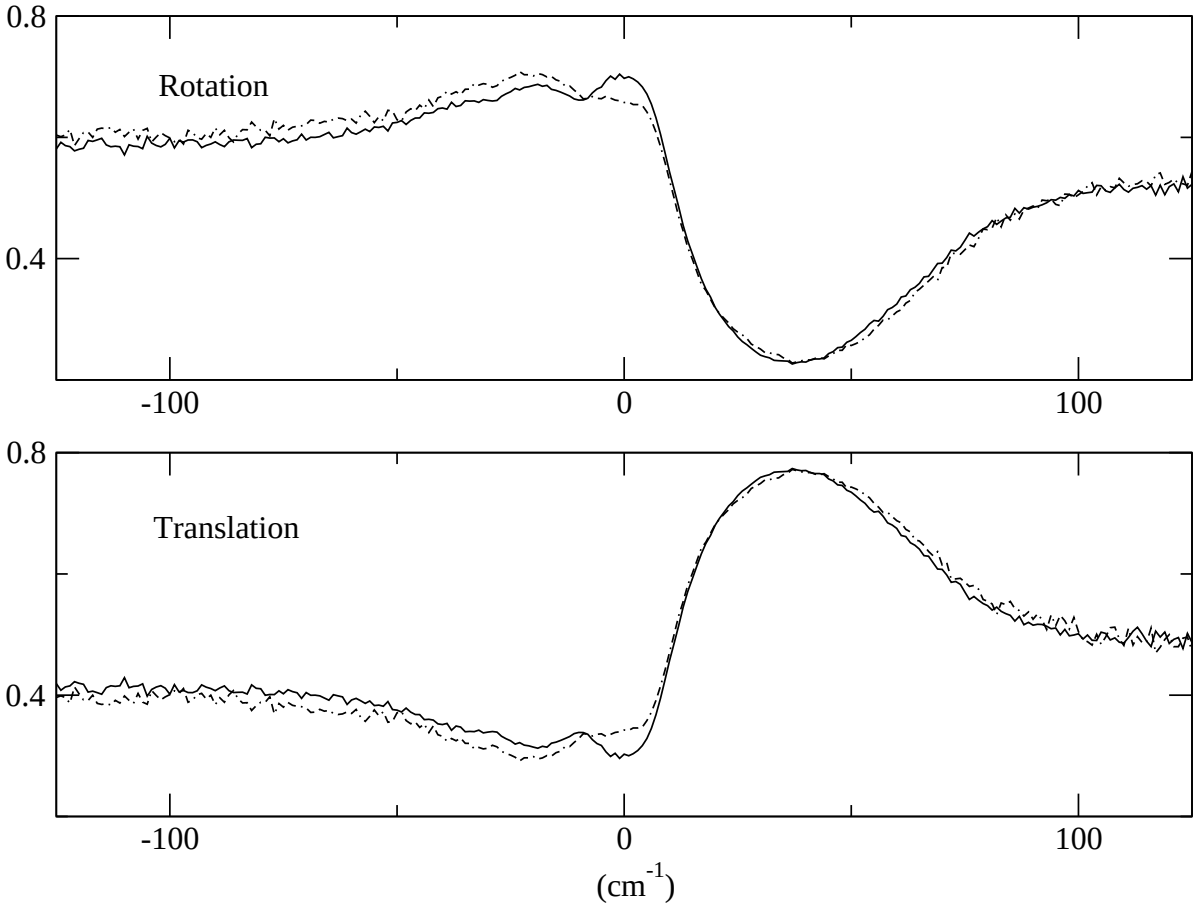

FIG. 3.4. Translational and rotational projectors of motion for two molten salts, with a solid line for the symmetric model and the dashed line for the asymmetric model.

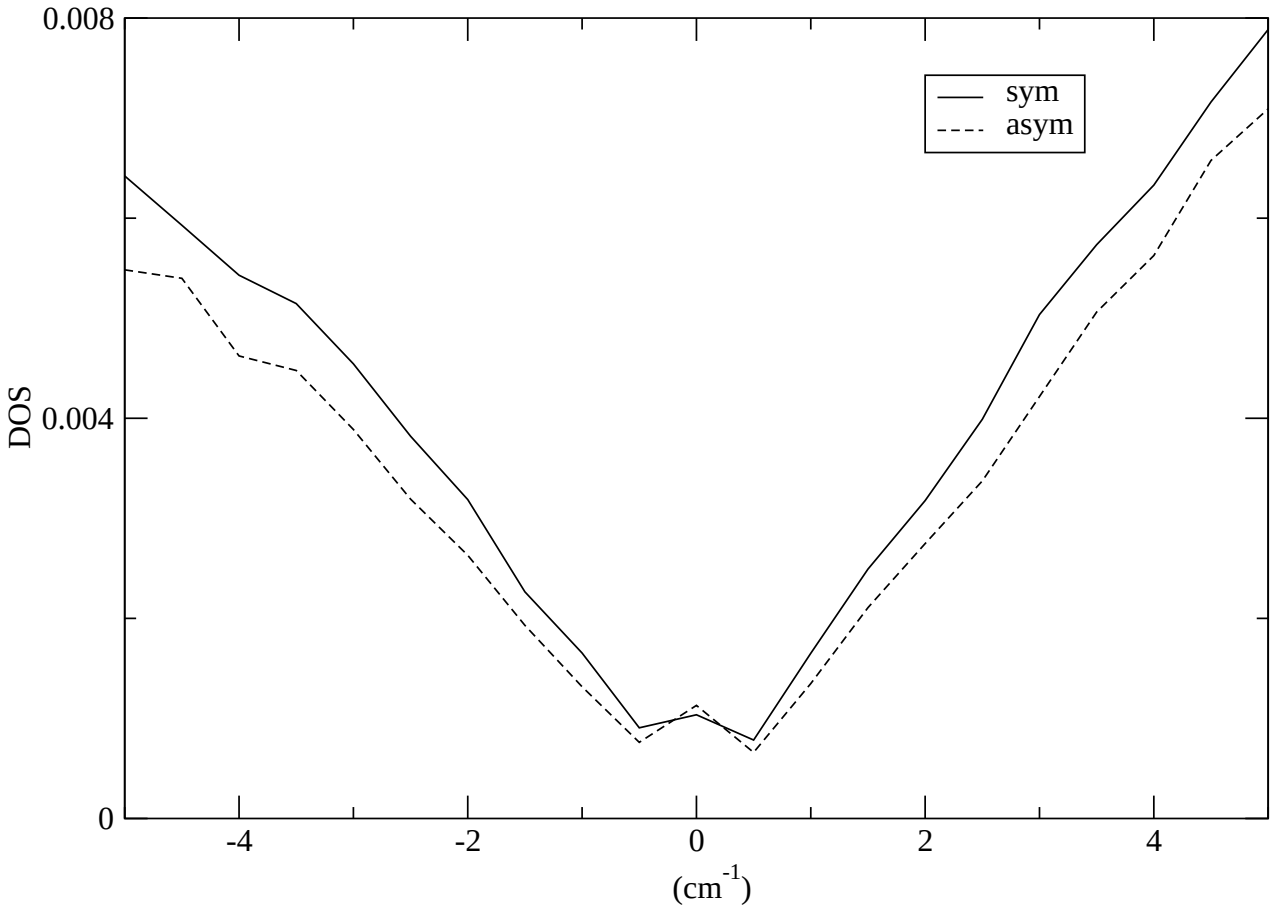

FIG. 3.5. Total density of states for two molten salts at zero frequency, with a solid line for the symmetric model and the dashed line for the asymmetric model.

CONCLUSION

In this thesis, we have presented a theoretical study of ionic liquids using a combination of analytical theory and molecular dynamics simulations methods.

We first introduced the definition of ionic liquids and their properties. A short review of recent research on ILs has been reported. In order to investigate the structure-property relationship of ionic liquids, we develop a descriptor called the Charge Lever Moment(CLM) related to the distributions of charge and mass in an ion based on the center of charge principle. We show that the value of the maximum CLM of an ion correlates strongly with the viscosity of an IL made from that ion. However, this CLM formalism breaks down for highly flexible ions and for ions with certain structural features, such as branched aliphatic chains.

With the idea that the charge distribution and symmetry of an ion should have a profound effect on liquid dynamics, we performed a series of molecular dynamics (MD) simulations on ILs composed of rigid model ions possessing a high symmetry in mass distribution but varying symmetry in their charge distribution. A slower librational decay and faster translational diffusion appear in the asymmetric species. This indicates stronger Coulomb interactions coupling rotational and translational motion in asymmetric species, consistent with our earlier work on the CLM formalism.

The study of the same model ions mentioned above was extended through the performance of an instantaneous normal mode (INM) analysis. The INM spectrum was assembled, and the separate translational and rotational contribution to each instantaneous normal mode analyzed by computing the appropriate projectors from their eigenvectors. We found that the INM densities of states are extremely similar except in the region near ω=0. The observed differences in the translational and rotational spectra in that region are consistent

with the expectations from MD simulations, and imply that this region of the spectrum is associated with diffusive transport.

REFERENCES

[1] Abbott, A. P.; Capper, G.; Davies, D. L.; Rasheed, R. K.; and Tambyrajah, V. 2003. Novel solvent properties of choline chloride/urea mixtures. *Chem. Comm.* 70–71.

[2] Aki, S. N. V. K.; Scurto, A. M.; and Brennecke, J. F. 2006. Ternary phase behavior of ionic liquid(IL)-organic-CO_2 systems. *Ind. Eng. Chem. Res.* 45:5574–5585.

[3] Angell, C. A. 1984. Strong and fragile liquids. In Ngai, K. L., and Wright, G. B., eds., *Relaxation in Complex Systems*. Washington, D. C.: Naval Research Laboratory. 3–11.

[4] Arzhantsev, S.; Ito, N.; Heitz, M.; and Maroncelli, M. 2003. Solvation dynamics of coumarin 153 in several classes of ionic liquids: Cation dependence of the ultrafast component. *Chem. Phys. Lett.* 381:278–286.

[5] Arzhantsev, S.; Jin, H.; Ito, N.; and Maroncelli, M. 2006. Observing the complete solvation response of DCS in imidazolium ionic liquids, from the femtosecond to the nanosecond regimes. *Chem. Phys. Lett.* 417:524–529.

[6] Baranyai, A.; Ruff, I.; and McGreevy, R. L. 1986. Monte Carlo simulation of the complete set of molten alkali halides. *J. Phys. C: Solid State* 19:453–465.

[7] Becke, A. D. 1993. Density-functional thermochemistry III. the role of exact exchange. *J. Chem. Phys.* 98:5648–5652.

[8] Berg, R. W. 2007. Raman spectroscopy and ab initio model calculations on ionic liquids. *Monat. Chemie* 138:1045–1075.

[9] Breneman, C. M., and Wiberg, K. B. 1990. Determining atom-centered monopoles

from molecular electrostatic potentials: The need for high sampling density in formamide conformational analysis. *J. Comp. Chem.* 11:361–373.

[10] Cang, H.; Li, J.; and Fayer, M. D. 2003. Orientational dynamics of the ionic organic liquid 1-ethyl-3-methylimidazolium nitrate. *J. Chem. Phys.* 119:13017–13022.

[11] Canongia-Lopes, J. N., and Pádua, A. A. H. 2006. Nanostructural organization in ionic liquids. *J. Phys. Chem. B* 110:3330–3335.

[12] Canongia-Lopes, J. N.; Deschamps, J.; and Pádua, A. A. H. 2004. Modeling ionic liquids using a systematic all-atom force field. *J. Phys. Chem. B* 108:2038–2047.

[13] Canongia-Lopes, J. N.; Gomes, M. F. C.; and Pádua, A. A. H. 2006. Nonpolar, polar, and associating solutes in ionic liquids. *J. Phys. Chem. B* 110:16816–16818.

[14] Chauvin, Y., and Olivier-Bourbigou, H. 1995. Nonaqueous ionic liquids as reaction solvents. *Chemtech* 25:26–30.

[15] Chelli, R.; Cardini, G.; and Califano, S. 1997. A molecular dynamics study of translation-rotation coupling in the NaCN plastic crystal. *J. Chem. Phys.* 107:8041–8050.

[16] Crosthwaite, J. M.; Aki, S. N. V. K.; Maginn, E. J.; and Brennecke, J. F. 2005a. Liquid phase behavior of imidazolium-based ionic liquids with alcohols: Effect of hydrogen bonding and non-polar interactions. *Fluid Phase Equil.* 228-229:303–309.

[17] Crosthwaite, J. M.; Muldoon, M. J.; Dixon, J. K.; Anderson, J. L.; and Brennecke, J. F. 2005b. Phase transition and decomposition temperatures, heat capacities and viscosities of pyridinium ionic liquids. *J. Chem. Thermo.* 37:559–568.

[18] Deeg, F. W.; Stankus, J. J.; Greenfield, S. R.; Newell, V. J.; and Fayer, M. D. 1989. Anisotropic reorientational relaxation of biphenyl: Transient grating optical kerr effect measurements. *J. Chem. Phys.* 90:6893.

[19] Del Pópolo, M. G., and Voth, G. A. 2003. On the structure and dynamics of ionic liquids. *J. Phys. Chem. B* 108:1744–1752.

[20] Dupont, J.; de Souza, R. F.; and Suarez, P. A. Z. 2002. Ionic liquid (molten salt) phase organometallic catalysis. *Chem. Rev.* 102:3667–3692.

[21] Dyson, P. J.; Ellis, D. J.; and Welton, T. 2001. A temperature-controlled reversible ionic liquid – water two phase-single phase protocol for hydrogenation catalysis. *Can. J. Chem.* 79:705–708.

[22] Earle, M. J.; Esperança, J. M. S. S.; Gilea, M. A.; Canongia-Lopes, J. N.; Rebelo, L. P. N.; Magee, J. W.; Seddon, K. R.; and Widegren, J. A. 2006. The distillation and volatility of ionic liquids. *Nature* 439:831–834.

[23] Eike, D. M.; Brennecke, J. F.; and Maginn, E. J. 2003. Predicting melting points of quaternary ammonium ionic liquids. *Green Chem.* 5:323–328.

[24] Engel, R.; Cohen, J. I.; and Lall, S. I. 2002. A new category of liquid salt: Liquid ionic phosphates (LIPs). *Phosphorus, Sulfur and Silicon* 177:1441–1445.

[25] Engkvist, O., and Karlström, G. 1997. Monte Carlo simulation study of short poly(ethylene oxide) chains at different concentrations. *J. Phys. Chem. B* 101:1631–1633.

[26] Forester, T., and Smith, W. 1994. On multiple time step algorithms and the Ewald sum. *Molecular Simulation* 13:195–304.

[27] Fox, D. M.; Gilman, J. W.; DeLong, H. C.; and Trulove, P. C. 2005. TGA decomposition kinetics of 1-butyl-2,3-dimethylimidazolium tetrafluoroborate and the thermal effects of contaminants. *J. Chem. Thermo.* 37:900–905.

[28] Frisch, M. J.; Trucks, G. W.; Schlegel, H. B.; Scuseria, G. E.; Robb, M. A.; Cheeseman, J. R.; Montgomery, J. A.; Vreven, T.; Kudin, K. N.; Burant, J. C.; Millam, J. M.; Iyengar, S. S.; Tomasi, J.; Barone, V.; Mennucci, B.; Cossi, M.; Scalmani, G.; Rega, N.; Petersson, G. A.; Nakatsuji, H.; Hada, M.; Ehara, M.; Toyota, K.; Fukuda, R.; Hasegawa, J.; Ishida, M.; Nakajima, T.; Honda, Y.; Kitao, O.; Nakai, H.; Klene, M.; Li, X.; Knox, J. E.; Hratchian, H. P.; Cross, J. B.; Adamo, C.; Jaramillo, J.; Gomperts, R.; Stratmann, R. E.; Yazyev, O.; Austin, A. J.; Cammi, R.; Pomelli, C.; Ochterski, J. W.; Ayala, P. Y.; Morokuma, K.; Voth, G. A.; Salvador, P.; Dannenberg, J. J.; Zakrzewski, V. G.; Dapprich, S.; Daniels, A. D.; Strain, M. C.; Farkas, O.; Malick, D. K.; Rabuck, A. D.; Raghavarchari, K.; Foresman, J. B.; Ortiz, J. V.; Cui, Q.; Baboul, A. G.; Clifford, S.; Cioslowski, J.; Stefanov, B. B.; Liu, G.; Liashenko, A.; Piskorz, P.; Komaromi, L.; Martin, R. L.; Fox, D. J.; Keith, T.; Al-Laham, M. A.; Peng, C. Y.; Nanayakkara, A.; Challacombe, M.; Gill, P. M. W.; Johnson, B.; Chen, W.; Wong, M. W.; Gonzalez, C.; and Pople, J. A. 2003. *GAUSSIAN03*. Pittsburgh, PA: Gaussian, Inc.

[29] Giraud, G.; Gordon, C. M.; Dunkin, I. R.; and Wynne, K. 2003. The effects of anion and cation substitution on the ultrafast solvent dynamics of ionic liquids: A time-resolved optical Kerr-effect spectroscopic study. *J. Chem. Phys.* 119:464–477.

[30] Gomes, M. F. C., and Pádua, A. A. H. 2003. Interactions of carbon dioxide with liquid fluorocarbons. *J. Phys. Chem. B* 107:14020–14024.

[31] Hajime, M.; Hikari, S.; and Kuniaki, T. 2005. preparation of room temperature

ionic liquids based on aliphatic onium cations and asymmetric amide anions and their electrochemical properties as a lithium battery electrolyte. *J. Pow. Sources* 146:45–50.

[32] Hänggi, P.; Talkner, P.; and Borkovec, M. 1990. Reaction-rate theory: Fifty years after Kramers. *Rev. Mod. Phys.* 62:251–333.

[33] Hanke, C. G., and Lynden-Bell, R. M. 2003. A simulation study of water-dialkylimidazolium ionic liquid mixtures. *J. Am. Chem. Soc.* 107:10873–10878.

[34] Hanke, C. G.; Price, S. L.; and Lynden-Bell, R. M. 2001. Intermolecular potentials for simulations of liquid imidazolium salts. *Mol. Phys.* 99:801–809.

[35] Hayashi, S.; Ozawa, R.; and Hamaguchi, H. 2003. Raman spectra, crystal polymorphism, and structure of a prototype ionic liquid [BMIM]Cl. *Chem. Lett.* 32:498–499.

[36] Holbrey, J. D.; Reichert, W. M.; Nieuwenhuyzen, M.; Johnston, S.; Seddon, K. R.; and Rogers, R. D. 2003. Crystal polymorphism in 1-butyl-e-methylimidazolium halides: Supporting ionic liquid formation by inhibition of crystallization. *Chem. Comm.* 1636–1637.

[37] Hu, Z., and Margulis, C. J. 2006a. Heterogeneity in a room-temperature ionic liquid: Persistent local environments and the red-edge effect. *Proc. Nat. Acad. Sci.* 103:831–836.

[38] Hu, Z., and Margulis, C. J. 2006b. A study of the time-resolved fluorescence spectrum and red edge effect of ANF in a room-temperature ionic liquid. *J. Phys. Chem. B* 110:11025–11028.

[39] Hu, Z., and Margulis, C. J. 2007. On the response of an ionic liquid to external pertrubations and the calculation of shear viscosity. *J. Phys. Chem. B* 111:4705–5714.

[40] Huddleston, J. G.; Visser, A. E.; Reichert, W. M.; Willauer, H. D.; Broker, G. A.; and Rogers, R. D. 2001. Characterization and comparison of hydrophilic and hydrophobic room temperature ionic liquids incorporating the imidazolium cation. *Green Chem.* 3:156–164.

[41] Hyun, B.-R.; Dzyuba, S. V.; Bartsch, R. A.; and Quitevis, E. L. 2002. Intermolecular dynamics of room-temperature ionic liquids: Femtosecond optical Kerr effect measurements on 1-alkyl-3-methylimidazolium Bis((trifluoromethyl)sulfonyl)imides. *J. Phys. Chem. A* 106:7579–7585.

[42] J.D.Gezelter; E.Rabani; and B.J.Berne. 1997. Can imaginary instantaneous nomal mode predict the barriers to self-diffusion. *J. Chem. Phys.* 107:12.

[43] J.E.Adams, and R.Stratt. 1990. Liquid theory for band structure in a liquid. ii. p-orbitals and phonons. *J. Chem. Phys.* 93:1332.

[44] Karelson, M. 2000. *Molecular Descriptors in QSAR/QSPR*. New York: Wiley-Interscience.

[45] Katayanagi, H.; Hayashi, S.; Hamaguchi, H.; and Nishikawa, K. 2004. Structure of an ionic liquid, 1-n-butyl-3-methylimidazolium iodide, studied by wide-angle X-ray scattering and Raman spectroscopy. *Chem. Phys. Lett.* 392:460–464.

[46] Kauffman, G. W., and Jurs, P. C. 2001. Prediction of surface tension, viscosity and thermal conductivity for common organic solvents using quantitative structure-property relationships. *J. Chem. Inf. Comput. Sci.* 41:408–418.

[47] Kobrak, M. N., and Sandalow, N. 2006. An electrostatic interpretation of structure-property relationships in ionic liquids. In Mantz, R. A., ed., *Molten Salts XIV*. Pennington, NJ: The Electrochemical Society.

[48] Kobrak, M. N. 2006. Characterization of the solvation dynamics of an ionic liquid via molecular dynamics simulation. *J. Chem. Phys.* 125:064502.

[49] Kobrak, M. N. 2007. A comparative study of solvation dynamics in room temperature ionic liquids. *J. Chem. Phys.* 127:184507.

[50] Kobrak, M. N. 2008. The chemical environment of ionic liquids: Links between liquid structure, dynamics and solvation. *Adv. Chem. Phys.* 139:85–176.

[51] Ladanyi, B. M., and Stratt, R. M. 1995. Short-time dynamics of solvation: Linear solvation theory for polar solvents. *J. Phys. Chem.* 99:2502–2511.

[52] Lee, C.; Yang, W.; and Parr, R. G. 1988. Development of the Colle-Salvetti correlation-energy formula into a functional of electron density. *Phys. Rev. B* 37:785.

[53] Li, H., and Kobrak, M. N. 2009. A molecular dynamics study of the influence of ionic charge distribution on the dynamics of a molten salt. *J. Chem. Phys.* 131:194507.

[54] Li, W.-X., and T.keyes. 1997. Three-flavor instataneous normal modes formalism: diffusion, harmonicity, and the potential energy landscape of liquids cs2. *J. Chem. Phys.* 108:252.

[55] Li, J.; Wang, I.; Fruchey, K.; and Fayer, M. D. 2006. Dynamics in supercooled ionic organic liquids and mode coupling theory analysis. *J. Phys. Chem. A* 110:10384–10391.

[56] Li, H.; Ibrahim, M.; Agberemi, I.; and Kobrak, M. N. 2008. The relationship between ionic structure and viscosity in room-temperature ionic liquids. *J. Chem. Phys.* 129:124507.

[57] Lynden-Bell, R. M.; McDonald, I. R.; and Klein, M. L. 1983. Analysis of translation-rotation coupling in an orientationally disordered ionic crystal. *Mol. Phys* 48:1093–1117.

[58] MacFarlane, D. R.; Meakin, P.; Amini, N.; and Forsyth, M. 1999. Pyrrolidinium imides: A new family of molten salts and conductive plastic crystal phases. *J. Phys. Chem. B* 103:4164–4170.

[59] MacFarlane, D. R.; Forsyth, S. A.; Golding, J.; and Deacon, G. B. 2002. Ionic liquids based on the imidazolium, ammonium, and pyrrolidinium salts of the dicyanamide ion. *Green Chem.* 4:444–448.

[60] Mandal, P. K.; Sarkar, M.; and Samanta, A. 2004. Excitation-wavelength-dependent fluorescence behavior of some dipolar molecules in room-temperature ionic liquids. *J. Phys. Chem. A* 108:9048–9053.

[61] Mantz, R. A., and Trulove, P. C. 2002. Viscosity and density of ionic liquids. In Wasserscheid, P., and Welton, T., eds., *Ionic Liquids in Synthesis*. Weinheim, Germany: Wiley-VCH. 56–68.

[62] Margulis, C. J.; Stern, H. A.; and Berne, B. J. 2002. Computer simulation of a "green chemistry" room-temperature ionic solvent. *J. Phys. Chem. B* 106:12017–12021.

[63] Matsuda, H.; Yamamoto, H.; Kurihara, K.; and Tochigi, K. 2007. Computer-aided reverse design for ionic liquids by QSPR using descriptors of group contribution type for ionic conductivities and viscosities. *Fluid Phase. Equil.* 261:434–443.

[64] Matsumoto, H.; Kageyama, H.; and Miyazaki, Y. 2002. Room temperature ionic liquids based on small aliphatic ammonium cations and asymmetric amide anions. *Chem. Commun.* 1726–1726.

[65] M.Buchner; B.M.Ladanyi; and R.Stratt. 1992. The short time dynamics of molecular liquids. *J. Chem. Phys.* 97:11.

[66] M.Buchner; B.M.Ladanyl; and R.M.Stratt. 1992. The short-time dynamics of molecular liquids.inm theory. *J. Chem. Phys.* 97:11.

[67] M.Cho; G.R.Fleming; and R.M.Stratt. 1994. Instanteous normal mode analysis of liquid water. *J. Chem. Phys.* 100:6672.

[68] Noda, A.; Hayamizu, K.; and Watanabe, M. 2001. Pulsed-gradient spin-echo ^{1}h and ^{1}9f NMR ionic diffusion coefficient, viscosity, and ionic conductivity of non-chloroaluminate room-temperature ionic liquids. *J. Phys. Chem. B* 105:4603–4610.

[69] Okada, I. 2001. Transport properties of molten salts. In Bockris, J. O.; Conway, B. E.; and White, R. E., eds., *Modern Aspects of Electrochemistry No. 34*. New York: Kluwer Academic/Plenum Publishers. 119–203.

[70] Olivier-Bourbigou, H., and Magna, L. 2002. Ionic liquids: Perspectives for organic and catalytic reactions. *J. Mol. Catal. A: Chemical* 182-183:419–437.

[71] Rebelo, L. P. N.; Canongia-Lopes, J. N.; Esperança, J. M. S. S.; and Filipe, E. 2005. On the critical temperature, normal boiling point and vapor pressure of ionic liquids. *J. Phys. Chem. B* 109:6040–6043.

[72] Ribeiro, M. C. C., and Madden, P. A. 1997. Instantaneous normal mode prediction for cation and anion diffusion in ionic melts. *J. Chem. Phys.* 106:8616–8619.

[73] Ribeiro, M. C. C.; de Oliveira, L. F. C.; and Gonçalves, N. S. 2001. Boson peak in the room-temperature molten salt tetra(*n*-butyl)ammonium croconate. *Phys. Rev. B* 63:104303–1 – 104303–8.

[74] R.Stratt. 1995. The instataneous normal modes of liquids. *Acc.Chem.Res.* 28:201.

[75] Ruhman, S.; Williams, L. R.; Joly, A. G.; Kohler, B.; and Nelson, K. A. 1987. Non-relaxational inertial motion in carbon disulfide liquid observed by femtosecond time-resolved impulsive stimulated scattering. *J.Phys.Chem.* 91:2237.

[76] Sangster, M. J. L., and Dixon, M. 1976. Interionic potentials in alkali halides and their use in simulations of the molten salts. *Adv. Phys.* 25:247–342.

[77] Sastry, S.; Debenedetti, P. G.; and Stillinger, F. H. 1998. Signatures of distinct dynamical regimes in the energy landscape of a glass-forming liquid. *Nature* 393:554–557.

[78] S.D.Bembenek, and B.B.Laird. 1996. The role of localization in glasses and supercooled liquids. *J. Chem. Phys.* 104:5199.

[79] Seddon, K. R. 1997. Ionic liquids for clean technology. *J. Chem. Tech. Biotechnol.* 68:351–356.

[80] Seddon, K. R. 2005. Ionic liquids database. *Chem. Int.* 27:23.

[81] Shah, J. K.; Brennecke, J. F.; and Maginn, E. J. 2002. Thermodynamic properties of the ionic liquid 1-n-butyl-3-methylimidazolium hexafluorophosphate from Monte Carlo simulations. *Green Chem.* 4:112–118.

[82] Shigeto, S., and Hamaguchi, H. 2006. Evidence for mesoscopic local structures in ionic liquids: CARS signal spatial distribution of Cnmim[PF_6]. *Chem. Phys. Lett.* 427:329–332.

[83] Shirota, H., and Castner, E. W. 2005a. Physical properties and intermolecular dynamics of an ionic liquid compared with its isoelectronic neutral binary solution. *J. Phys. Chem. A* 109:9388–9392.

[84] Shirota, H., and Castner, E. W. 2005b. Why are viscosities lower for ionic liquids with -$CH_2Si(CH_3)_3$ vs -$CH_2C(CH_3)_3$ substitutions on the imidazolium cations? *J. Phys. Chem. B* 109:21576–21585.

[85] Shirota, H.; Funston, A. M.; Wishart, J. F.; and Castner, E. W. 2005. Ultrafast dynamics of pyrrolidinium cation ionic liquids. *J. Chem. Phys.* 122:184512/1–12.

[86] Smith, W., and Forester, T. R. 2001. *The DL_POLY2 User Manual*. Daresbury, England: Daresbury Laboratory.

[87] S.Ryu, and R.Stratt. 2004. A case study in the molecular interpretation of optical kerr effect spectra. *J.Phys.Chem.* 108:6782.

[88] Stratt, R. M., and Cho, M. 1994. The short-time dynamics of solvation. *J. Chem. Phys.* 100:6700–6708.

[89] Sun, J.; Forsyth, M.; and MacFarlane, D. R. 1998. Room-temperature molten salts based on the quaternary ammonium ion. *J. Phys. Chem. B* 102:8858–8864.

[90] Suzuki, T.; Ebert, R.-U.; and Schüürmann, G. 2001. Application of neural networks to modeling and estimating temperature-dependent liquid viscosity of organic compounds. *J. Chem. Inf. Comput. Sci.* 41:776–790.

[91] T.Keyes. 1994. Unstable modes in supercooled and normal liquids. *J. Chem. Phys.* 101:6.

[92] T.Keyes. 1997. Instataneous normal modes approach to liquid state dynamics. *J.Phys.Chem.* 101:2921.

[93] Tokuda, H.; Hayamizu, K.; Ishii, K.; Susan, M. A. B. H.; and Watanabe, M. 2005. Physicochemical properties and structures of room temperature ionic liquids. 2. Variation of alkyl chain length in imidazolium cation. *J. Phys. Chem. B* 109:6103–6110.

[94] Tokuda, H.; Ishii, K.; Susan, M. A. B. H.; Tsuzuki, S.; Hayamizu, K.; and Watanabe, M. 2006. Physicochemical properties and structures of room temperature ionic liquids. 3. Variation of cationic structures. *J. Phys. Chem. B* 110:2833–2839.

[95] Trullás, J., and Padró, J. A. 1997. Diffusive transport properties in monovalent and divalent metal-ion halide melts: A computer simulation study. *Phys. Rev. B* 55:12210–12217.

[96] Trullás, J.; Giró, A.; Padró, J. A.; and Silbert, M. 1991. Charge ordering and size effects in sodium chloride and copper chloride melts: A computer simulation study. *Physica A* 171:384–402.

[97] Urahata, S. M., and Ribeiro, M. C. C. 2004. Structure of ionic liquids of 1-alkyl-3-methylimidazolium cations: A systematic comparative simulation study. *J. Chem. Phys.* 120:1855–1863.

[98] Urahata, S. M., and Ribeiro, M. C. C. 2005. Single particle dynamics in ionic liquids of 1-alkyl-3-methylimidazolium cations. *J. Chem. Phys.* 122:024511/1–9.

[99] Urahata, S. M., and Ribeiro, M. C. C. 2006. Collective excitations in an ionic liquid. *J. Chem. Phys.* 124:074513.

[100] Valkenburg, M. E. V.; Vaughn, R. L.; Williams, M.; and Wilkes, J. S. 2005. thermochemistry of ionic liquid heat-transfer fluids. *Thermochim. Acta* 425:181–188.

[101] Varnek, A.; Kireeva, N.; Tetko, I. V.; Baskin, I. I.; and Solovév, V. P. 2007. Exhaustive QSPR studies of a large, diverse set of ionic liquids: How accurately can we predict melting points? *J. Chem. Inf. Model.* 47:1111–1122.

[102] Wang, Y., and Voth, G. A. 2005. Unique spatial heterogeneity in ionic liquids. *J. Am. Chem. Soc.* 127:12192–12193.

[103] Wang, Y., and Voth, G. A. 2006. Tail aggregation and domain diffusion in ionic liquids. *J. Phys. Chem. B* 110:18601–18608.

[104] Wangsness, R. K. 1986. *Electromagnetic Fields*. New York: John Wiley & Sons, 2nd. edition.

[105] Wasserscheid, P., and Welton, T. 2002. *Ionic Liquids in Synthesis*. Mörlenbach, Germany: Wiley-VCH.

[106] Welton, T. 1999. Room-temperature ionic liquids for synthesis and catalysis. *Chem. Rev.* 99:2071–2083.

[107] Xiao, D.; Rajian, J. R.; Li, S.; Bartsch, R. A.; and Quitevis, E. L. 2006. Additivity of optical Kerr effect spectra of binary ionic liquid mixtures: Implications for nanostructural organization. *J. Phys. Chem. B* 110:16174–16178.

[108] Xu, W.; Cooper, E. I.; and Angell, C. A. 2003. Ionic liquids: Ion mobilities, glass temperatures, and fragilities. *J. Phys. Chem. B* 107:6170–6178.

[109] Yan, T.; Burnham, C. J.; Del Pópolo, M. G.; and Voth, G. A. 2004. Molecular dynamics simulation of ionic liquids: The effect of electronic polarizability. *J. Phys. Chem. B* 108:11877–11881.

[110] Zhou, Z.; Matsumoto, H.; and Tatsumi, K. 2006. Cyclic quaternary ammonium ionic liquids with perfluoroalkyltrifluoroborates: Synthesis, characterization and properties. *Chem. Eur. J.* 12:2196–2212.

[111] Zwanzig, R. 1983. On the relation between self-diffusion and viscosity of liquids. *J. Chem. Phys.* 79:4507.